

1 **Mapping Asian anthropogenic emissions of**
2 **non-methane volatile organic compounds to multiple**
3 **chemical mechanisms**

4
5 **M. Li^{1,2}, Q. Zhang¹, D. G. Streets³, K. B. He², Y. F. Cheng⁴, L. K. Emmons⁵,**
6 **H. Huo⁶, S. C. Kang², Z. Lu³, M. Shao⁷, H. Su⁴, X. Yu⁸, and Y. Zhang⁹**

7
8 [1]{Ministry of Education Key Laboratory for Earth System Modeling, Center for
9 Earth System Science, Tsinghua University, Beijing, China}

10 [2]{State Key Joint Laboratory of Environment Simulation and Pollution Control,
11 School of Environment, Tsinghua University, Beijing, China}

12 [3]{Decision and Information Sciences Division, Argonne National Laboratory,
13 Argonne, IL, USA}

14 [4]{Multiphase Chemistry Department, Max Planck Institute for Chemistry, Mainz,
15 Germany}

16 [5]{Atmospheric Chemistry Division, National Center for Atmospheric Research,
17 Boulder, CO, USA}

18 [6]{Institute of Energy, Environment and Economy, Tsinghua University, Beijing,
19 China}

20 [7]{State Key Joint Laboratory of Environmental Simulation and Pollution Control,
21 College of Environmental Sciences and Engineering, Peking University, Beijing,
22 China}

23 [8]{Beijing Green Resource Research Co. Ltd., Beijing, China}

24 [9]{Department of Marine, Earth and Atmospheric Sciences, North Carolina State
25 University, Raleigh, North Carolina, USA}

26

27

28

29 Correspondence to: Q. Zhang (qiangzhang@tsinghua.edu.cn)

30 **Abstract**

31 An accurate speciation mapping of non-methane volatile organic compounds
32 (NMVOC) emissions has an important impact on the performance of chemical
33 transport models (CTMs) in simulating ozone mixing ratios and secondary organic
34 aerosols. Taking the INTEX-B Asian NMVOC emission inventory as the case, we
35 developed an improved speciation framework to generate model-ready anthropogenic
36 NMVOC emissions for various gas-phase chemical mechanisms commonly used in
37 CTMs in this work, by using an explicit assignment approach and updated NMVOC
38 profiles. NMVOC profiles were selected and aggregated from a wide range of new
39 measurements and the SPECIATE database v4.2. To reduce potential uncertainty from
40 individual measurements, composite profiles were developed by grouping and
41 averaging source profiles from the same category. The fractions of oxygenated volatile
42 organic compounds (OVOC) were corrected during the compositing process for those
43 profiles which used improper sampling and analyzing methods. Emissions of
44 individual species were then lumped into species in different chemical mechanisms
45 used in CTMs by applying mechanism-dependent species mapping tables, which
46 overcomes the weakness of inaccurate mapping in previous studies. Emission
47 estimates for individual NMVOC species differ between one and three orders of
48 magnitude for some species when different sets of profiles are used, indicating that
49 source profile is the most important source of uncertainties of individual species
50 emissions. However, those differences are diminished in lumped species as a result of
51 the lumping in the chemical mechanisms. Gridded emissions for eight chemical
52 mechanisms at 30 min \times 30 min resolution as well as the auxiliary data are available
53 at: <http://mic.greenresource.cn/intex-b2006>. The framework proposed in this work can
54 be also used to develop speciated NMVOC emissions for other regions.

55 **1. Introduction**

56 Non-methane volatile organic compounds (NMVOCs) include a variety of
57 chemical species that can be emitted from biomass burning, biogenic, and
58 anthropogenic sources (Guenther et al., 2012; Piccot et al., 1992; van der Werf et al.,
59 2010). NMVOCs are of great concern because they play a key role in tropospheric
60 chemistry as precursors of ozone and secondary organic aerosols (SOA) and many
61 NMVOC species do damage to human health. NMVOCs differ significantly in their
62 impacts on ozone and SOA formation, and these differences need to be represented
63 appropriately in chemical transport models (CTMs). Such CTMs have been used to
64 guide the development of emission control strategies by governmental agencies (e.g.,
65 US EPA, 2007; Wang et al., 2010; Xing et al., 2011), predict the effects of changes of
66 emissions on the formation of ozone and SOA (e.g., Hogrefe et al., 2004; Y. Zhang et
67 al., 2010, 2013), and study the sensitivity of the model predictions of pollutant
68 concentrations to different gas-phase chemical mechanisms (e.g., Kim et al., 2011;
69 Zhang et al., 2012).

70 In CTMs, atmospheric chemical reactions are usually characterized by a specific
71 chemical mechanism, in which many individual NMVOC species are lumped together
72 according to similarities in chemical structure or reactivity. The most commonly used
73 chemical mechanisms in CTMs include: the State Air Pollution Research Center 1999
74 version (SAPRC-99, Carter, 2000) and an updated version SAPRC-07 (Carter, 2010);
75 Carbon Bond Mechanism version IV (CB-IV, Grey et al., 1989) and two variants with
76 updates in reactions and related kinetic data including the Carbon Bond Mechanism
77 version Z (CBMZ, Zaveri and Peters, 1999) and CB05 (Yarwood et al., 2005); as well
78 as the second generation Regional Acid Deposition Model chemical mechanism
79 (RADM2, Stockwell et al., 1990) and its variants with updates in reactions and related
80 kinetic data including the Regional Atmospheric Chemistry Mechanism (RACM,
81 Stockwell et al., 1997) and RACM2 (Goliff et al., 2013). This has been a challenge to
82 map speciated NMVOC emissions data with organic compounds treated in different

83 chemical mechanisms through a translation scheme from total NMVOC emissions to
84 lumped, model-ready emissions. In the US National Emission Inventory system, The
85 Sparse Matrix Operator Kernel Emissions (SMOKE) modeling system has been
86 developed with the function of preparing model-ready NMVOC emissions as inputs for
87 any chemical mechanisms (e.g., CB05, SAPRC-99, RADM2) used in CTMs. In the
88 SMOKE model, total NMVOC emissions are first split into individual species by
89 assigning appropriate source profiles from the US EPA's SPECIATE database (Hsu and
90 Divita, 2009; Simon et al., 2010) using source classification codes, and then
91 aggregated to lumped model species treated in different chemical mechanisms using
92 corresponding mechanism-dependent mapping tables (Houyoux et al., 2000).

93 For the Asian region, although speciated NMVOC emissions have been estimated
94 by various regional and global inventories (e.g., Klimont et al., 2002; Streets et al.,
95 2003; Ohara et al., 2007; Bo et al., 2008; Wei et al., 2008), the interfaces between
96 NMVOC emissions and CTMs remain underdeveloped. Table 1 summarizes the
97 existing global and regional NMVOC emission inventories covering Asia. In addition
98 to the known uncertainties in estimates for the total NMVOC emission budget, there are
99 two other major weaknesses in Asian emission inventory datasets. First, most
100 inventory datasets are not ready for model input. Although many global and regional
101 inventories provide emissions of chemical species groups for Asia, based on reactivity
102 and structure similarity (see Table 1), those species groups differ from lumped model
103 species used in chemical mechanisms. The mapping process between species in
104 inventories and models was usually performed by modelers without a standard
105 procedure, which may lead to inaccuracies and introduce unpredictable uncertainties.
106 This is especially true for a lumped-structure mechanism (e.g., carbon bond mechanism)
107 where organics are grouped by chemical bond type (Fu et al., 2009). Second, recent
108 local measurements on NMVOC source profiles have not been updated in most
109 inventory studies. It is believed that NMVOC source profiles vary among regions
110 worldwide as the consequence of differences in fuel quality and combustion conditions.

111 For example, NMVOC composition from vehicles in China has been shown to be
112 significantly different from those in the US (Liu et al., 2008a). Recognizing this
113 problem, there are increasing numbers of measurements for local NMVOC source
114 profiles in Asia. They cover many of the most important sources, such as residential
115 fuel combustion (Tsai et al., 2003; Liu et al., 2008a; Wang et al., 2009), solvent use (Liu
116 et al., 2008a; Yuan et al., 2010), petrochemical industry (Liu et al., 2008a), on-road
117 transportation (Liu et al., 2008a; Lai et al., 2009), and fuel evaporation (Y. L. Zhang et
118 al., 2013). However, only some of these locally measured profiles have been used in
119 recent NMVOC emission inventories that covered part of China (Zheng et al., 2009) or
120 the transportation sector in China (Cai and Xie, 2007). An updated Asian NMVOC
121 emission database with state-of-the-art profiles is still missing.

122 In support of the US NASA Intercontinental Chemical Transport
123 Experiment-Phase B (INTEX-B) mission, we developed an air pollutant emission
124 inventory for Asia for the year 2006 (Zhang et al., 2009), including speciated
125 NMVOC emissions as model-ready inputs for various chemical mechanisms (i.e.,
126 SAPRC-99, SAPRC-07, CB-IV, CB05, and RADM2), processed by an explicit
127 speciation assignment approach. In the INTEX-B inventory, emissions for individual
128 VOC species are first calculated for each source category by applying profiles from
129 local measurements and the SPECIATE database, and individual species were lumped
130 to emitted species in different chemical mechanisms by corresponding species
131 mapping tables. The emissions dataset for the SAPRC-99 mechanism is available to
132 the public from <http://mic.greenresource.cn/intex-b2006> and has been widely used in
133 CTMs (e.g., Wang et al., 2011; Lin et al., 2012; Dong et al., 2013).

134 Although the step-by-step speciation process used in the INTEX-B inventory has
135 provided model-ready NMVOC emission data to the community and reduced the
136 uncertainties associated with inaccurate speciation mapping procedure, there remain
137 many unresolved issues. Two major weaknesses are associated with profile selection
138 and processing and need to be addressed. First, the INTEX-B profiles omit some

139 important species, particularly oxygenated volatile organic compounds (OVOCs).
140 OVOCs, which include alcohols, aldehydes, ketones and ethers, play a key role in
141 atmospheric organic chemistry and many of them are known to have a detrimental
142 effect on human health (Christian et al., 2004; Fu et al., 2008; Hopkins et al., 2003).
143 The magnitude of OVOCs is significant and cannot be neglected for OVOC-rich
144 emitting sources, such as biofuel burning and diesel vehicle exhaust (Andreae and
145 Merlet, 2001; Schauer et al., 1999, 2001). Second, a single profile is assigned to each
146 specific source, which may introduce inaccuracy into the speciation process due to the
147 limitation of profiles (Cai and Xie, 2007; Reff et al., 2009). One limitation is that for
148 sources containing multiple fuels and technologies, such as biofuel combustion, a
149 single profile cannot represent the overall emission characteristics. On the other hand,
150 the quality of profiles is difficult to quantify and may introduce unpredictable levels
151 of uncertainty during profile selection.

152 In order to narrow the uncertainty from profile selection and processing
153 mentioned above, we followed the speciation framework of the INTEX-B inventory
154 but with necessary profile adjustments for OVOC-rich sources and the development
155 of composite profiles in this work. We also evaluated the impact of profile update on
156 the speciated emissions and ozone production, which is useful in understanding the
157 uncertainties in emission speciation and determining the source of discrepancies
158 between “bottom-up” emission inventories and “top-down” constraints (e.g., from
159 in-situ measurements and satellite observations).

160 This paper is organized as follows. Sect. 2 summarizes the methods and data that
161 were used in this work and the INTEX-B inventory, including total NMVOC
162 emissions, profile development, ozone formation potentials (OFPs) calculation,
163 mechanism species mapping, and spatial allocation. Sect. 3 presents and compares the
164 emissions of individual species and lumped mechanism species estimated in this work
165 and the original INTEX-B inventory. In Sect. 4, the sensitivity of emissions and OFPs
166 to profile selection is analyzed and the effects of updated profiles are assessed by

167 comparing OFPs calculated from the two estimates. Perspectives for future work are
168 discussed in Sect. 5.

169

170 **2. Methodology and data**

171 The general approach of speciation is to multiply total NMVOC emissions by a
172 corresponding chemical speciation profile for each source type. Figure 1 presents the
173 flow diagram of the methodology used in this work, as applied to the INTEX-B
174 inventory. In this work, we start from total NMVOC emission estimates for 2006 in
175 the INTEX-B Asian inventory (Zhang et al., 2009), select and aggregate profiles from
176 both local measurements and the SPECIATE database v.4.2 (Hsu and Divita, 2009),
177 and apply them to split total NMVOC into individual species. Compared to the
178 INTEX-B inventory, the main difference of this work is the use of composite profiles.
179 OFPs are calculated to evaluate the effect of profile update on ozone formation based
180 on the speciated NMVOC emissions developed in this work. Individual species are
181 lumped into model species of different mechanisms by specific mapping tables.
182 Finally, gridded emissions are developed at 30 min \times 30 min resolution using various
183 spatial proxies.

184 **2.1 NMVOC emissions in 2006 for Asia**

185 Total NMVOC emissions were obtained from the 2006 Asian emission inventory
186 for the NASA INTEX-B mission (Zhang et al., 2009). This inventory is an update of
187 the TRACE-P Asian NMVOC inventory developed for an earlier NASA mission
188 (Streets et al., 2003) with significant improvement for China using detailed activity
189 data and local emission factors. The improved methodology for China led to a higher
190 degree of source specificity in China than other Asian countries. To compile a
191 speciated NMVOC emission dataset with consistent and comparable methodology for
192 all of Asia, a set of 55 source categories was aggregated by grouping similar source
193 types for China and other Asian regions. Anthropogenic NMVOC emissions for 2006

194 for each source category are tabulated in Table S1. As estimated in the INTEX-B
195 inventory, emissions from China (23.2 Tg) dominate total emissions in Asia (42% of
196 total), followed by Southeast Asia (14.1 Tg, 26%) and India (10.8 Tg, 20%).

197 Figure 2 presents the NMVOC emissions by eight sectors for China, Other regions
198 of East Asia, India, Other regions of South Asia and Southeast Asia. For all of Asia,
199 residential combustion, on-road transportation and industrial non-combustion
200 contribute most to the total emissions, whereas the sector distributions vary
201 significantly for different regions. For China, these three sectors share equally,
202 whereas industrial non-combustion dominates the emissions for Other East Asia. The
203 shares of residential combustion and on-road transportation are significant both for
204 India and Other South Asia. For Southeast Asia, the emissions of total NMVOC are
205 dominated by residential combustion and on-road transportation.

206 **2.2 Development and assignment of source profiles**

207 After classifying the INTEX-B total NMVOC emissions into grouped source
208 categories, the next step is to assign or create a profile for each source. For a given
209 source category, the profile development and assignment involve three steps: (1)
210 search candidate profiles, both from the SPECIATE database v.4.2 and local
211 measurements; (2) revise profiles that do not contain an OVOC contribution for
212 OVOC-rich sources; and (3) construct “composite” profile if more than one profile is
213 available.

214 The profiles are selected with the following steps. We first searched candidate
215 profiles from SPECIATE database v.4.2 and a variety of literatures for each source
216 category. The SPECIATE v4.2 database provides the most comprehensive collection
217 of available NMVOC profiles, containing more than 1600 source profiles from
218 measurements mainly in the US (Simon et al., 2010). Because the fuel quality,
219 combustion technology and emission regulations in Asia often differ significantly
220 from those in the US, profiles taken from the SPECIATE database may not represent

221 the chemical characteristics of sources accurately (Zheng et al., 2009). To develop a
222 database of state-of-the-art profiles for Asia, local profiles for each emitting source
223 type were gathered from the literature where available. As the numbers of
224 local-measured profiles are still very limited, we include all available “local” profiles
225 from literatures as candidate profiles. For those sources which local profiles are
226 available and we believe that there are significant differences between Asian and
227 western countries due to different technologies and/or legislations, only local profiles
228 are used (e.g. solvent use). For sources which similar technologies are used in Asian
229 and western countries (e.g., boilers, vehicles), profiles from SPECIATE database are
230 also included. In order to reduce the uncertainties associated with profile selection in
231 the original INTEX-B speciation process, as mentioned in Sect. 1, we take steps 2 and
232 3 respectively to solve the “OVOC” and “single profile” issue. We identified the
233 OVOC rich sources and corrected the incomplete profiles which missed OVOC
234 fraction. The “composite” profile for each source was finally developed with the same
235 weighting factor for each individual candidate profile. The specific procedure is
236 described below.

237 **2.2.1 Inclusion of OVOC in profiles**

238 From a comprehensive review of available profiles, we found that OVOCs
239 contribute a large fraction of total NMVOC emissions from biofuel combustion and
240 diesel vehicles (Schauer et al., 1999, 2001; Andreae and Merlet, 2001). However,
241 OVOC fractions are missing in some profiles for these two sources due to sampling
242 and analysis approaches (e.g., Liu et al., 2008a). Often, NMVOC samples were
243 collected by canisters and then analyzed by gas chromatographic (GC) techniques,
244 such as GC-mass spectrometry (GC-MS), GC-flame ionization detection (GC-FID),
245 and GC-electron capture detection (GC-ECD). These techniques have proved to be
246 accurate for determining the levels of hydrocarbons, but they are not suitable for
247 analyzing carbonyl species because they cannot quantify unstable and “sticky”
248 compounds accurately (Christian et al., 2004). Carbonyls are best analyzed by proton

249 transfer mass spectrometry (PTR-MS) online monitoring (Christian et al., 2004) or
250 collected by 2,4-dinitrophenylhydrazine (DNPH)-impregnated C18 cartridges and
251 then analyzed by high-performance liquid chromatography with UV detection
252 (HPLC/UV) (Schauer et al., 1999, 2001; Huang et al., 2011).

253 Until now, a standard protocol for NMVOC sampling and analysis is still not well
254 developed. Many local-measured profiles used canisters to collect samples and GC
255 techniques to analyze NMVOC species (e.g., Tsai et al., 2003; Liu et al., 2008a). In
256 this work, we still include those profiles in the speciation process after correcting their
257 OVOC fractions, as local-measured profiles are believed to better represent the
258 real-world conditions. The general procedure of the revision is to append “OVOC” as
259 a component to the original profile along with their percentage contribution calculated
260 from profiles with OVOC measured for the same source. The fraction of each species
261 except “OVOC” in the revised profile is calculated as:

$$262 \quad X_{revised}(i, j) = \frac{X_{ori}(i, j)}{\sum_j X_{ori}(i, j)} \times (1 - \overline{X_{ovoc}(i, j)}) \quad (1)$$

263 Where i is the emitting source; j is the NMVOC species; $X_{ori}(i, j)$ and $X_{revised}(i, j)$ are
264 the fractions of species j in the original and revised profiles of emission source i ,
265 respectively; X_{ovoc} is the proportion of OVOC for each selected profile that has OVOC
266 measured for source i ; and $\overline{X_{ovoc}}$ is the calculated mean of X_{ovoc} . The mass fraction of
267 unspatiated “OVOC” in the revised profile is labeled with “missing value”, not
268 involved in the speciation process.

269 Figure 3 demonstrates inclusion of the missing OVOC fraction for the crop
270 residue combustion profile measured by Liu et al. (2008). The average OVOC
271 fraction, calculated as 28.9% according to the four profiles that include OVOC
272 (Andreae and Merlet, 2001; Wang et al., 2009; and Profile No. 4420 and No. 4421 in
273 SPECIATE v.4.2), is used to scale the original profile proportionally. Inclusion of
274 OVOC fraction for diesel vehicle profiles is illustrated in Fig. S1. The revised profiles,
275 along with other selected profiles, are then added to the profile database, ready for the

276 next step of the speciation process.

277 **2.2.2 Development of composite profiles**

278 A “composite” profile is created for sources where multiple candidate profiles are
279 available. For a given source category, species along with their mass fractions in each
280 candidate profile are grouped and averaged, excluding missing values. It should be
281 noted that the OVOC fractions in incomplete profiles are determined to be missing
282 values, not involved in the calculation of average value. We choose median instead of
283 mean as average to help mitigate possible large errors stemming from the presence of
284 outlier samples and measurements (Reff et al., 2009). After the grouping and
285 averaging process, the “composite” profile is scaled to 100% proportionally. The
286 grouping and averaging process can reduce the uncertainties the empirical selection of
287 profiles. However, it may introduce additional uncertainties from the assumption that
288 each candidate profile for the same source is weighting equally.

289 Here we take the development of a composite profile for biofuel combustion as
290 an example. Eleven profiles for crop residue and wood combustion were selected and
291 processed into a composite profile, as listed from P1 to P11 in Fig. 4. The top 30
292 species and their corresponding fractions are presented, accounting for 84% of the
293 total mass in the composite profile. As shown in Fig. 4, measurements of species
294 exhibit a large diversity among profiles. First, none of these species are contained in
295 all profiles. In spite of the fact that species such as ethene, benzene and propane are
296 included in most of the profiles, the fractions for some species are only included in
297 one or two profiles (e.g., phenanthrene, glyoxal, and acetone), which introduces large
298 uncertainties in the composite profile. Second, for specific species, fractions from
299 different profiles vary significantly, revealing the discrepancies caused by different
300 fuels and technologies of the emitting source and/or different samples and techniques
301 used in the profile measurements. Thus, using a single profile will generate
302 considerably different emissions for individual species, indicating the huge
303 uncertainty associated with profile selection and application. The profile development

304 method used in this work, by selecting and averaging multiple profiles, is an
305 important way to reduce this uncertainty.

306 A complete list of profiles used in this work is presented in Table S1. The
307 composited profiles developed in this work are available from the following website:
308 <http://mic.greenresource.cn/intex-b2006>. The individual profiles for diesel vehicles
309 and the composite profile are illustrated in Fig. S2 as another example. After the
310 profile-assignment speciation, region- and source-specific speciated NMVOC
311 emissions for around 700 individual species are processed in this work, comprising
312 the basic emission dataset for lumping into different chemical mechanisms and OFPs
313 analysis.

314 **2.3 Calculation of OFPs**

315 The ozone reactivities for various NMVOC species differ significantly, which can
316 be scaled by the Maximum Incremental Reactivity (MIR) (Carter, 1994). OFP has
317 been widely used in assessing the roles of NMVOC emissions in ozone formation and
318 guiding the development of cost-effective ozone control measures (e.g., Song et al.,
319 2007; Zheng et al., 2009), which can be estimated based on mass and MIR for each
320 species. OFPs for individual species are calculated by multiplying emissions by
321 corresponding MIR values:

$$322 \quad OFP(i, j, k) = EVOC(i, k) \times X(i, j) \times MIR(j) \quad (2)$$

323 Where $OFP(i, j, k)$ is the ozone formation potential of species j in region k , emitted
324 from source i ; $EVOC(i, k)$ is the emission of total NMVOC for source i in region k ;
325 $X(i, j)$ is the fraction of species j from the profile for source i , which is taken from
326 the composite profiles developed in this work; $MIR(j)$ is the maximum incremental
327 reactivity scale for species j . OFPs by chemical groups and by sectors are calculated
328 by summing up OFP values by corresponding individual species, to evaluate the
329 ozone formation potentials of different chemical groups and sectors. It should be
330 noted that species with no MIR values were ignored during the calculation of OFPs.

331 This treatment will introduce uncertainties in evaluating the magnitude of OFPs but
332 could be negligible when comparing the differences of identified compounds in this
333 work.

334 **2.4 Assignments for different chemical mechanisms**

335 In atmospheric models, individual VOC emissions are usually assigned to “lumped”
336 species in a simplified mechanism to balance the accuracy and computational
337 efficiency, according to the similarities of their chemical reactivity. In this work,
338 emission assignments for various chemical mechanisms are calculated by multiplying
339 the emissions of individual species by species- and mechanism-specific conversion
340 factors as follows:

$$341 \quad EVOC(i, k, m) = \sum_{j=1}^n \left[\frac{EVOC(i, k) \times X(i, j)}{mol(j)} \times C(j, m) \right] (3)$$

342 Where k is the region; m is species type in a mechanism; n represents the number of
343 species emitted from source i . $EVOC$ is the total NMVOC emissions; $X_{i,j}$ is the mass
344 fraction of species j to total NMVOC emissions for source i , which is obtained from
345 the composite profiles; $mol(j)$ is the mole weight of species j ; and $C_{j,m}$ is the conversion
346 factor of species j for mechanism category m . In this work, the conversion factors were
347 taken from the mechanism-dependent mapping tables developed by Carter (2013).

348 For some profiles, a fraction of total NMVOC is assigned as “unknown” or
349 “undefined” species, which probably reflects the unidentified fraction arising from the
350 limitation of the analysis technique (Schauer et al., 1999). In this work, we treated the
351 “unknown” species as a single species during the composite profile development and
352 then assigned emissions from “unknown” species mainly into ALK5, NROG, OLE1,
353 ARO1, and ARO2 in the SAPRC-99 mechanism and PAR, UNR, OLE, TOL, XYL,
354 and ALDX in CB05, according to Carter (2013). However, the “unknown” species is
355 not included in the OFP calculation, as its maximum incremental reactivity is
356 undefined.

357 Emissions for six chemical mechanisms are calculated in this work based on the
358 availability of mapping tables in Cater (2013): CB-IV, CB05, SAPRC-99, SAPRC-07,
359 RADM2 and RACM2. These mapping tables are available at
360 <http://www.engr.ucr.edu/~carter/emitdb/>. In these tables, each individual organic
361 compound is assigned with conversion factors to mechanism species according to its
362 carbon bond (for CBIV and CB05) and chemical group (for SAPRC-99, SAPRC-07,
363 RADM2, and RACM2); hence it provides a consistent way of species mapping for
364 different chemical mechanisms. To our knowledge, this is the most accurate chemical
365 mapping approach in the community, which has been used in processing US emission
366 inventories. We also calculated emissions for two global models, GEOS-Chem and
367 MOZART-4, by lumping SAPRC-99 species to emission species in those two global
368 models. The mapping tables from SAPRC-99 species to GEOS-Chem and MOZART-4
369 species are presented in Tables 2 and 3 and the abbreviations of those species are
370 provided in Tables A1-A4.

371 **2.5 Spatial allocation**

372 Emissions are gridded for CTMs and aggregated into four sectors (power, industry,
373 residential and transportation), both by individual species and by chemical
374 mechanisms. We followed the top-down approach used in the INTEX-B inventory
375 (Zhang et al., 2009) to distribute country- or provincial-level emissions to grids using
376 various spatial proxies at 1 km × 1 km resolution (Streets et al., 2003; Woo et al., 2003).
377 Spatial proxies used in this work include: total population data extracted from
378 LandScan Global Population Dataset developed by Oak Ridge National Laboratory
379 (ORNL, 2004), urban and rural population data developed from partitioning total
380 population using urban land cover from LandScan 2000 database (ORNL, 2002), and
381 road networks from the Digital Chart of the World (DCW, 1993).

382 Table 4 listed the spatial proxies used in this work. All power generation units
383 with capacity larger than 300MW in China are identified as large point sources, while

384 other plants are treated as area sources and distributed by total population. Urban
385 population was used for distributing emissions from industrial combustion, residential
386 coal-fired boilers; rural population was used for residential biofuel combustion and
387 off-road transportation; road networks were used for on-road transportation emissions;
388 and total population was used for all other area sources. The final gridded emissions
389 were aggregated to 30 min × 30 min resolution.

390 **3. Results**

391 **3.1 Speciated NMVOC Emissions by individual species**

392 Using the approaches described in Sect. 2, emissions of ~700 individual NMVOC
393 species for Asia are estimated for the year 2006. Figure 5 presents emissions of the 30
394 species with the highest OFPs for the whole Asian region. These top 30 species
395 contributed 44% to total Asian anthropogenic NMVOC emissions and 82% to total
396 OFPs. For species with small emissions, the emission estimates have high uncertainty
397 due to the inaccuracy of the emission profiles and omission of minor emitting source
398 types.

399 As shown in Fig. 5, the order of OFPs of the top 30 species differs significantly
400 from that of emissions (by mass), which is attributed to the variation of chemical
401 reactivity of species, scaled by MIR in this work. Emphasis is placed on OVOCs and
402 alkenes with high MIRs and relatively high contribution to OFPs. It is interesting to
403 notice that some OVOCs, such as glyoxal and methylglyoxal, are determined to have
404 high OFPs but relatively low emission estimates, due to their high reactivity scales.
405 Alkanes and some aromatics (e.g., benzene) tend to be less chemically reactive in the
406 atmosphere and have lower contribution to OFPs compared to their emissions.

407 Figure 5 also shows the distribution of individual species emissions among major
408 contributing source types (by fuel type and by sector). Gasoline and biofuel
409 combustion are two common significant contributing sources for most species, with
410 the exception of a high proportion of contribution from non-combustion sources for

411 aromatics (e.g., 34% for xylene, 54% for toluene). Ethene is the largest contributor to
412 ozone formation potential (29.0 Tg-O₃) with the second highest emissions (3.2 Tg),
413 coming mainly from biofuel combustion (1.2 Tg, 38% of total), gasoline combustion
414 (1.0 Tg, 32%), coal combustion (0.3 Tg, 10%), and non-combustion sources (0.3 Tg,
415 10%). Alkenes other than ethene such as propene, 2-methyl-2-butene, 1-butene also
416 have significant contributions to OFPs. Propene is the third largest contributor to
417 ozone formation, having similar distribution by fuel and sector as ethene. Important
418 aromatic ozone precursors include xylenes, toluene, and 1,2,4-trimethylbenzene. We
419 estimate that xylene emissions in Asia in 2006 were 3.4 Tg (27.2 Tg-O₃ ozone
420 formation potential), ranking first in terms of magnitude of emissions and second in
421 terms of OFPs.

422 As shown in Fig. 5, glyoxal, formaldehyde, methylglyoxal, acetaldehyde, and
423 ethyl alcohol are OVOC species with remarkable contributions to anthropogenic
424 OFPs over Asia. Some of OVOCs (e.g., glyoxal and methylglyoxal) also have
425 important contributions to SOA formation through aqueous-phase reactions in
426 aerosols and clouds (Carlton et al., 2007; Ervens and Volkamer, 2010). In this work,
427 primary glyoxal and methylglyoxal are mostly emitted from biofuel combustion.
428 However, it should be noted that incomplete profiles for other sources resulting from
429 inappropriate sampling and analysis methods are a potential source of high
430 uncertainty; newly measured profiles may provide additional sources of these OVOC
431 species in the future.

432 Figure 6 compares the emissions of individual species estimated in this work and
433 the original INTEX-B emission inventory, based on the same total NMVOC emission
434 estimates. A total of 425 species were presented in Fig. 6, covering the species with
435 annual emissions larger than 10 Mg in two inventories. Large differences are observed,
436 having a general pattern of more OVOC and alkenes emissions estimated from this
437 work than in the original INTEX-B inventory. For 132 species (31% of total), the
438 differences between the two estimates were within 100%, while emission estimates

439 for 60 species (14% of total) differ by one order of magnitude or more, implying that
440 large uncertainties are introduced from NMVOC source profiles. Considering that the
441 uncertainties associated with activity rates and total NMVOC emission factors are
442 usually less than 100% (Zhao et al., 2011), the source profiles could be recognized as
443 the most important source of uncertainties in emission estimates for individual
444 NMVOC species. This, in turn, has significant implications for the ability of CTMs to
445 reliably model the oxidizing nature of the Asian atmosphere.

446 Compared to the original INTEX-B inventory, this work estimated much lower
447 emissions for acetylene, but higher emissions for xylene and glyoxal (as shown in Fig.
448 S3). The significant decrease of acetylene emissions and increase of xylene and
449 glyoxal emissions are mainly due to the change of residential biofuel combustion
450 profile. As can be seen from Fig. 4, the profile used in the original INTEX-B
451 inventory is taken from Tsai et al. (2003) (P2 and P8), which contains high mass
452 fraction of acetylene (27.4% for P2 and 27.0% for P8, respectively) in contrast to the
453 composite profile.

454 For species like ethene, benzene and acetylene, emissions are lower than in the
455 INTEX-B inventory; whereas propene, xylene, glyoxal, acetone, and methyl alcohol
456 emissions are higher. Because alkenes, aromatics and OVOC are reactive precursors
457 for ozone and SOA formation, these differences in emissions may lead to
458 enhancements in OFPs and ozone and SOA concentrations simulated by CTMs. The
459 impact of emission differences from the speciation process on OFPs will be quantified
460 and discussed in the next section.

461 Figure 7 shows the spatial distribution of toluene emissions in 2006 at 30 min ×
462 30 min horizontal resolution. Gridded emissions for ~700 individual species at the
463 same resolution are all developed following the methodologies described in Sect. 2.5
464 and are available by request. These datasets would be useful for comparing with
465 in-situ measurements and identifying possible sources of uncertainties in emission
466 inventories (e.g., Wang et al., 2013). However, as emissions of some species may

467 differ by 1-3 orders of magnitude when assigning different sets of profiles, these
468 datasets should be used with caution in interpreting the discrepancy between
469 observations and NMVOC emissions, because the discrepancy may be attributed to
470 uncertainties in the profiles rather than in total NMVOC emissions.

471 **3.2 Speciated NMVOC emissions by chemical groups**

472 Figures 8 and 9 present 2006 NMVOC emissions in Asia by chemical groups
473 estimated in this work. We estimate that alkenes accounted for the largest share of
474 Asian total NMVOC emissions in 2006 (240 Gmole (10^9 mole), 30% of total),
475 followed by alkanes (191 Gmole, 24%), OVOCs (155 Gmole, 17%), aromatics (114
476 Gmole, 14%), and alkynes (56 Gmole, 7%). The shares from alkanes and aromatics
477 are larger in Japan and South Korea (Other East Asia) than in other regions, reflecting
478 the significant contribution from the industrial sector in the two countries.

479 We also compared emissions estimated in this work with the original INTEX-B
480 inventory by chemical groups in Figs. 8 and 9. In contrast to the large differences in
481 emission estimates for individual species, the discrepancies are reduced greatly after
482 grouping individual species into similar chemical functional groups. The emission
483 differences of alkanes, alkenes, and aromatics are within 5% between the original
484 INTEX-B inventory and this work, while significant differences were still found for
485 alkynes and OVOC emissions. A large increase compared to the original INTEX-B
486 inventory is observed for OVOC emissions, from 53 Gmoleyr^{-1} to 155 Gmoleyr^{-1} , in
487 contrast to the decrease of alkynes emissions from 261 Gmoleyr^{-1} to 56 Gmoleyr^{-1} .
488 Similar differences are found in all Asian regions except Other East Asia, where the
489 two estimates show similar distributions among chemical groups.

490 The dramatic increase for OVOC emissions and decrease for alkynes emissions is
491 dominated by the residential sector, mainly due to the creation and application of the
492 “composite” profile for biofuel combustion. The P2 and P8 profiles (both measured by
493 Tsai et al., 2003) that were used in the original INTEX-B speciation process are

494 incomplete profiles that miss the contributions from OVOCs. The increase of OVOC
495 emissions is due to the inclusion of the OVOC fraction in the “composite” profile.
496 Compared to P2 and P8, other candidate profiles have a much lower contribution from
497 acetylene (see Fig. 4), leading to the lower share of alkynes in the “composite” profile
498 used in this work. The inclusion of OVOC in incomplete profiles further decreases the
499 contributions for non-OVOC species, which also contribute to the differences in
500 alkyne contributions.

501 **3.3 Model-ready emissions**

502 One of the key objectives of this study is to develop model-ready NMVOC
503 emission datasets for Asian anthropogenic sources as the emission inputs for CTMs.
504 In this work, model-ready emissions for eight chemical mechanisms were developed:
505 CB-IV, CB05, SAPRC-99, SAPRC-07, RADM2, RACM2, GEOS-Chem, and
506 MOZART-4. Emissions for the GEOS-Chem model and MOZART-4 model were
507 converted from SAPRC-99 emissions using the species mapping tables presented in
508 Tables 2 and 3. Fig. 10 illustrates the 2006 Asian anthropogenic NMVOC emissions
509 lumped by SAPRC-99 and CB05 species. Emissions are then distributed by various
510 spatial proxies following the approaches described in Sect. 2.5 and aggregated at 30
511 min × 30 min resolution. Gridded emissions for the eight chemical mechanisms
512 mentioned above are all available from our website
513 (<http://mic.greenresource.cn/intex-b2006>). Gridded emissions are provided for four
514 sectors: power plants, industry, residential, and transportation. Those data can be used
515 directly as model inputs without further species mapping. As an example, Fig. 11
516 presents the map of OLE1 (a SAPRC-99 species) emissions by sector covering all
517 regions included in this work, showing a broad spatial distribution among residential,
518 transportation and industry sectors.

519 As individual species are usually highly lumped in CTMs, it is important to
520 investigate how the speciation process impacts emissions in lumped species in

521 different mechanisms. In Fig. 10, we compare the speciated emissions assignments by
522 the SAPRC-99 and CB05 mechanisms, both in the INTEX-B inventory and this study.
523 The differences in lumped species emissions between the original INTEX-B inventory
524 and this work are much smaller compared to individual species, indicating that the
525 uncertainties associated with profile selection and processing are diminished as a
526 result of the lumping in the chemical mechanisms.

527 However, there are still significant differences between the two estimates. For
528 SAPRC-99 species, sharp increases of OVOC and ARO2 emissions from the
529 residential sector are found, contrasting with a decrease of ETHE (ethene) and ALK2
530 (primarily propane and acetylene) emissions for the same sector. OLE1 and OLE2
531 emissions from the transportation sector are larger in this work, contributing to the
532 differences in the two estimates for those two species. These differences are mainly
533 attributed to the updated profiles of biofuel combustion and on-road vehicles. The
534 differences between the two estimates by CB05 species show similar patterns as the
535 SAPRC-99 species (although this was represented in different lumping species), while
536 PAR emissions agree well between the two estimates, due to a high degree of
537 lumping.

538 Figure 12 further presents emissions by SAPRC-99 species for each Asian region
539 and compares with the original INTEX-B estimates. As the emission characteristics
540 for Other South Asia are very close to India, we present emissions of South Asia as a
541 whole. For South Asia and Southeast Asia, where emissions are dominated by the
542 residential sector, the two estimates differ significantly in OVOC, ALK2, and ETHE
543 emissions due to updates of profiles in residential and transportation sector, as
544 discussed above. For Other East Asia, the differences between the two estimates are
545 smaller, because the NMVOC emissions are dominated by the industrial sector in
546 which similar profiles were used.

547

548 **4. Impacts of profile development on ozone production**

549 **4.1 Ozone Formation Potentials (OFPs)**

550 Given the fact that emission estimates of individual NMVOC emissions in Asia
551 are heavily influenced by source profiles, it is important to understand how the
552 variations in emission estimates then impact the prediction of ozone production.
553 Based on the emissions by individual species and corresponding MIR, OFPs of Asian
554 anthropogenic NMVOC emissions in 2006 are calculated by sector and chemical
555 groups, as presented in Fig. 13.

556 The total OFPs of 2006 Asian anthropogenic NMVOC emissions calculated in this
557 work are 195 Tg-O₃, 33% higher than the OFPs from the original INTEX-B inventory,
558 indicating that the compilation of NMVOC source profiles can significantly impact
559 estimates of ozone production. In this work, we estimated that alkenes have the
560 largest contribution to total OFPs (46%), followed by aromatics (28%), OVOC (18%),
561 alkanes (7%), and alkynes (1%). Alkenes and OVOCs have larger contributions to
562 total OFPs than to total emissions, while alkanes and alkynes have smaller
563 contributions to OFPs due to their relatively low MIR.

564 Compared to the INTEX-B inventory, higher OFP contributions from alkenes,
565 aromatics, and OVCs are estimated. Higher OFPs from alkenes are mainly because
566 the locally measured profiles included for the transportation and industrial sectors
567 have higher proportions of propene and butenes, which have larger MIR than ethene.
568 Ethene contributes 34% to the total OFPs of alkenes in our new estimates, much
569 lower than the 58% in the original INTEX-B inventory. For aromatics, the emission
570 increase from aromatics other than benzene, especially xylenes with high ozone
571 reactivity, accounts for the increase of OFP. The increased in the OFP contribution
572 from OVOCs can be attributed to higher estimates of aldehyde emissions from the
573 residential sector. Note that total OFPs from the residential sector are almost the same
574 between the two estimates, which is mainly due an offsetting of the increase in

575 emissions of OVOC by a decrease in emissions of alkenes.

576 **4.2 Sensitivity analysis of individual profiles**

577 Since significant differences in emissions and OFPs are observed between the
578 original INTEX-B inventory and this work, which is attributed to the update of profile
579 selection and compilation, it is worth examining the sensitivity of individual profiles
580 to emission estimates and OFPs. From the analysis presented above, we found that the
581 profiles for biofuel combustion and on-road vehicles contributed significantly to those
582 differences. In this work, 11 biomass burning profiles covering different fuel types
583 and combustion conditions are used for compiling the “composite” profile of biofuel
584 combustion, as shown in Fig. 4. Emissions by individual species vary significantly
585 among these 11 profiles, which is partly due to the variation in fuel and combustion
586 types. When developing the Asian NMVOC emission inventory, such variations were
587 ignored by treating biofuel combustion as a single source category, due to the lack of
588 detailed statistics on fuel types and combustion conditions.

589 Based on the concept of MIR for individual species, we evaluate the ozone
590 reactivity scale for each profile by calculating OFPs per unit NMVOC emission, as
591 shown in Fig. 14, to determine the sensitivity of OFPs to source profiles. The profiles
592 from Andreae and Merlet (2001) (P1) and No. 4420 from the SPECIATE database
593 v.4.2 (P10) tend to produce more ozone when used in the speciation, because of the
594 high fractions of alkenes and OVOC, respectively. Since the OVOC fraction is
595 relatively high in P10, contributions to ozone formation from OVOC might be
596 overestimated if only P10 was used for biomass burning, whereas they may be
597 underestimated by using P2, P3, P6 or P7 (Tsai et al., 2003; Liu et al., 2008a), which
598 have no OVOC measured. The difference of OFP between the highest and the lowest
599 values from using different profiles is up to a factor of three, demonstrating the high
600 sensitivity of ozone formation to profiles. The composite profile represents the
601 average level of ozone formation for the biofuel combustion source.

602 We further compare the emissions of SAPRC-99 and CB05 species estimated with
603 those 11 different profiles and the composite profile, as presented in Fig. 15. It can be
604 seen that the standard deviations are very large for SAPRC-99, especially for ETHE
605 and ALK2, indicating that model simulations configured with SAPRC-99 mechanism
606 would be sensitive to profile selection. On the other hand, the variations in CB05
607 species are relatively small compared with SAPRC-99 species, which can be
608 explained by the high degree of lumping for CB05.

609 Sensitivity tests by both speciated emissions and ozone formation for diesel
610 vehicles are also performed, as showed in Fig. S4 and S5, drawing the same
611 conclusion that ozone formation potentials and model-ready emissions are very
612 sensitive to the profile selection and processing. The immediate implication is that
613 using a single profile will introduce large uncertainty into the speciation process, and
614 the composite profile developed in this work can combine the species information
615 from all profiles and represent the average emission characteristics of the emitting
616 source. Thus the uniform profile processing system that groups and aggregates
617 multiple profiles can reduce the uncertainty associated with profile selection,
618 especially when one-to-one mapping of emission source to profile is not feasible due
619 to the different degrees of source specificity.

620

621 **5. Discussion**

622 In this study, we developed a step-by-step assignment framework to map Asian
623 anthropogenic NMVOC emissions to eight chemical mechanisms used in different
624 CTMs. To our best knowledge, this is the first work providing model-ready NMVOC
625 emissions database over Asia. Compared to previous work, we used
626 mechanism-specific mapping tables from Carter (2013) to accurately assign
627 individual NMVOC emissions to species groups in different chemical mechanisms,
628 which avoided the uncertainties from the species mapping process. We also compiled
629 “composite” profiles where more than one profile was available for a given source

630 category, to reduce the uncertainties arising from conflicting individual measurements
631 and the empirical selection of profiles.

632 Although we believe that the uncertainties in model-ready emissions provided by
633 this work are reduced significantly through our approach, they are still high, mainly
634 due to inadequacies in source profiles. More local measurements with standard
635 source-specific sampling and analysis methods are needed to reduce the discrepancies
636 among different measurements and enhance the data quality of profiles. Another
637 remaining uncertainty in this work is the mismatch between profile and source
638 classification in inventories. The level of detail in source profile measurements is
639 usually higher than that in the source categories of bottom-up inventories. The
640 composite profiles combined from different measurements then imply a hidden
641 assumption that each profile has the same weighting factor in that source category,
642 which is not always true. In future work, more detailed source category classification
643 that balances the complexity and data availability would help to narrow the
644 uncertainties.

645 Top-down constraints from in-situ observations provide useful information for
646 understanding emissions of NMVOC species through correlations between species
647 (e.g., Barletta et al., 2008; Tang et al., 2008) or source apportionment models (e.g.,
648 Liu et al., 2008a,b; Wang et al., 2013). Since profiles are key factors both in receptor
649 models (e.g., the chemical mass balance model) and speciated NMVOC inventory
650 developments, the inconsistency between “receptor-oriented” and “bottom-up”
651 emission estimates may be caused by differences in profile selection to some degree,
652 which needs more analysis in future work. Recent advancements in satellite
653 observations provide additional constraints on NMVOC emissions through
654 formaldehyde and glyoxal column densities (Wittrock et al., 2006; Fu et al., 2007; Liu
655 et al., 2012). Using glyoxal observations from the SCIAMACHY satellite instrument,
656 Liu et al. (2012) concluded that the underestimated aromatics emissions in current
657 inventories are the most likely missing source of glyoxal. From this work, we found

658 that primary emissions of glyoxal from biomass burning might be another important
659 source. Integration of bottom-up inventories and satellite observations would help to
660 close the gap between emission inventories and observations in the future.

661

662 **Acknowledgements**

663 The work was supported by China's National Basic Research Program
664 (2010CB951803 and 2014CB441301), the National Science Foundation of China
665 (41222036 and 21221004), and the Tsinghua University Initiative Research Program
666 (2011Z01026). This work was partly sponsored by the US EPA STAR grant
667 R83337601 at Argonne National Laboratory and North Carolina State University.

668 Table A1. Description of SAPRC-99 NMVOC emitting species from anthropogenic
 669 sources^a.

Species in SAPRC-99	Description
ACET	Acetone
ALK1	Primarily ethane
ALK2	Primarily propane and acetylene
ALK3	Alkanes and other non-aromatic compounds that react only with OH, and have k_{OH} between 2.5×10^3 and $5 \times 10^3 \text{ ppm}^{-1} \cdot \text{min}^{-1}$
ALK4	Alkanes and other non-aromatic compounds that react only with OH, and have k_{OH} between 5×10^3 and $1 \times 10^4 \text{ ppm}^{-1} \cdot \text{min}^{-1}$
ALK5	Alkanes and other non-aromatic compounds that react only with OH, and have k_{OH} greater than $1 \times 10^4 \text{ ppm}^{-1} \cdot \text{min}^{-1}$
ARO1	Aromatics with $k_{OH} < 2 \times 10^4 \text{ ppm}^{-1} \cdot \text{min}^{-1}$
ARO2	Aromatics with $k_{OH} > 2 \times 10^4 \text{ ppm}^{-1} \cdot \text{min}^{-1}$
BACL	Biacetyl
BALD	Aromatic aldehydes (e.g., benzaldehyde)
CCHO	Methyl Hydroperoxide
CRES	Cresols
ETHE	Ethene
GLY	Glyoxal
HCHO	Formaldehyde
IPRD	Unsaturated aldehydes other than acrolein and methacrolein
MACR	Methacrolein
MEK	Ketones and other non-aldehyde oxygenated products which react with OH radicals slower than $5 \times 10^{-12} \text{ cm}^3 \text{ molec}^{-2} \cdot \text{sec}^{-1}$
MEOH	Methyl alcohol
MGLY	Methylglyoxal
MVK	Aromatic aldehydes (e.g., benzaldehyde)
NROG	Unreactive organic chemicals
NVOL	Nonvolatile organic chemicals
OLE1	Alkenes (other than ethene) with $k_{OH} < 7 \times 10^4 \text{ ppm}^{-1} \cdot \text{min}^{-1}$
OLE2	Alkenes with $k_{OH} > 7 \times 10^4 \text{ ppm}^{-1} \cdot \text{min}^{-1}$
PHEN	Phenol
PRD2	Ketones and other non-aldehyde oxygenated products which react with OH radicals faster than $5 \times 10^{-12} \text{ cm}^3 \text{ molec}^{-2} \cdot \text{sec}^{-1}$
RCHO	Lumped C3 ⁺ Aldehydes

670 ^a Source: Carter (2000).

671

672 Table A2. Description of CB05 NMVOC emitting species from anthropogenic
 673 sources^a.

Species in CB05	Description
ALD2	Acetaldehyde
ALDX	Propionaldehyde and higher aldehydes
ETH	Ethene
ETHA	Ethane
ETOH	Ethyl alcohol
FORM	Formaldehyde
IOLE	Internal olefin carbon bond (R-C=C-R)
MEOH	Methyl alcohol
NVOL	Nonvolatile organic chemicals
OLE	Terminal olefin carbon bond (R-C=C)
PAR	Paraffin carbon bond (C-C)
TOL	Toluene and other monoalkyl aromatics
UNR	Unreactive VOCs
XYL	Xylene and other polyalkyl aromatics

674 ^a Source: http://www.camx.com/files/cb05_final_report_120805.aspx.

675

676 Table A3. Description of GEOS-CHEM NMVOC emitting species from
 677 anthropogenic sources^a.

Species in GEOS-Chem	Description
ACET	Acetone
ALD2	Acetaldehyde
ALK4	Lumped \geq C4 Alkanes
C2H6	Ethane
C3H8	Propane
CH2O	Formaldehyde
MEK	Methyl Ethyl Ketone
PRPE	Lumped \geq C3 Alkenes

678 ^a Source: <http://acmg.seas.harvard.edu/geos/doc/man/>.

679

680 Table A4. Description of MAZART-4 NMVOC emitting species from anthropogenic
 681 sources^a.

Species for MOZART-4	Description
BIGALK	Lumped alkanes C > 3
BIGENE	Lumped alkenes C > 3
TOLUENE	Lumped aromatics
C3H6	Propene
C3H8	Propane
C2H6	Ethane

C2H4	Ethene
MEK	Methyl ethyl ketone
CH2O	Formaldehyde
CH3CHO	Acetaldehyde
CH3COCH3	Acetone
CH3OH	Methyl alcohol
C2H5OH	Ethyl alcohol

682 ^a Source: Emmons et al. (2010).

683

684 **References**

- 685 Andreae, M. O., and Merlet, P.: Emission of trace gases and aerosols from biomass
686 burning, *Glob. Biogeochem. Cy.*, 15, 955-966, doi: 10.1029/2000GB001382,
687 2001.
- 688 Barletta, B., Meinardi, S., Simpson, I. J., Zou, S., Sherwood Rowland, F., and Blake,
689 D. R.: Ambient mixing ratios of nonmethane hydrocarbons (NMHCs) in two
690 major urban centers of the Pearl River Delta (PRD) region: Guangzhou and
691 Dongguan, *Atmos. Environ.*, 42, 4393-4408, 2008.
- 692 Bo, Y., Cai, H., and Xie, S. D.: Spatial and temporal variation of historical
693 anthropogenic NMVOCs emission inventories in China, *Atmos. Chem. Phys.*, 8,
694 7297-7316, doi: 10.5194/acp-8-7297-2008, 2008.
- 695 Boeke, N. L., Marshall, J. D., Alvarez, S., Chance, K. V., Fried, A., Kurosu, T. P.,
696 Rappengluck, B., Richter, D., Walega, J., Weibring, P., and Millet, D. B.:
697 Formaldehyde columns from the Ozone Monitoring Instrument: Urban versus
698 background levels and evaluation using aircraft data and a global model, *J.*
699 *Geophys. Res.*, 116, D05303, doi: 10.1029/2010JD014870, 2011.
- 700 Cai, H. and Xie, S.: Estimation of vehicular emission inventories in China from 1980
701 to 2005, *Atmos. Environ.*, 41, 8963-8979, 2007.
- 702 Carlton, A. G., Turpin, B. J., Altieri, K. E., Seitzinger, S., Reff, A., Lim, H.-J., and
703 Ervens, B.: Atmospheric oxalic acid and SOA production from glyoxal: Results of
704 aqueous photooxidation experiments, *Atmos. Environ.*, 41, 7588-7602, 2007.
- 705 Carter, W. P. L.: Development of ozone reactivity scales for volatile organic
706 compounds, *J. Air Waste Manage.*, 44, 881-899, 1994.
- 707 Carter, W. P. L.: Documentation of the SAPRC-99 chemical mechanism for VOC
708 reactivity assessment, report to the California Air Resources Board, available at:
709 <http://www.engr.ucr.edu/~carter/reactdat.htm> (last access: October 2013), 2000.
- 710 Carter, W. P. L.: Development of the SAPRC-07 chemical mechanism, *Atmos.*
711 *Environ.*, 44, 5324-5335, 2010.

712 Carter, W. P. L.: Development of an improved chemical speciation database for
713 processing emissions of volatile organic compounds for air quality models, report
714 available at: <http://www.engr.ucr.edu/~carter/emitdb/> (last access: November
715 [2013](#)), 2013.

716 Christian, T. J., Kleiss, B., Yokelson, R. J., Holzinger, R., Crutzen, P. J., Hao, W. M.,
717 Shirai, T., and Blake, D. R.: Comprehensive laboratory measurements of
718 biomass-burning emissions: 2. First intercomparison of open-path FTIR, PTR-MS,
719 and GC-MS/FID/ECD, *J. Geophys. Res.*, 109, D02311, doi:
720 10.1029/2003JD003874, 2004.

721 Dong, X., Gao, Y., Fu, J. S., Li, J., Huang, K., Zhuang, G., and Zhou, Y.: Probe into
722 gaseous pollution and assessment of air quality benefit under sector dependent
723 emission control strategies over megacities in Yangtze River Delta, China, *Atmos.*
724 *Environ.*, 79, 841-852, 2013.

725 Duffy, B. L., Nelson, P. F., Ye, Y., and Weeks, I. A.: Speciated hydrocarbon profiles
726 and calculated reactivities of exhaust and evaporative emissions from 82 in-use
727 light-duty Australian vehicles, *Atmos. Environ.*, 33, 291-307, 1999.

728 Duncan, B. N., Yoshida, Y., Olson, J. R., Sillman, S., Martin, R. V., Lamsal, L., Hu, Y.,
729 Pickering, K. E., Retscher, C., Allen, D. J., and Crawford, J. H.: Application of
730 OMI observations to a space-based indicator of NO_x and VOC controls on surface
731 ozone formation, *Atmos. Environ.*, 44, 2213-2223, 2010.

732 Emmons, L. K., Walters, S., Hess, P. G., Lamarque, J. F., Pfister, G. G., Fillmore, D.,
733 Granier, C., Guenther, A., Kinnison, D., Laepple, T., Orlando, J., Tie, X., Tyndall,
734 G., Wiedinmyer, C., Baughcum, S. L., and Kloster, S.: Description and evaluation
735 of the Model for Ozone and Related chemical Tracers, version 4 (MOZART-4),
736 *Geosci. Model Dev.*, 3, 43-67, doi: 10.5194/gmd-3-43-2010, 2010.

737 Ervens, B. and Volkamer, R.: Glyoxal processing by aerosol multiphase chemistry:
738 towards a kinetic modeling framework of secondary organic aerosol formation in
739 aqueous particles, *Atmos. Chem. Phys.*, 10, 8219-8244, doi:

740 10.5194/acp-10-8219-2010, 2010.

741 Fu, J. S., Streets, D. G., Jang, C. J., Hao, J. M., He, K. B., Wang, L. T., and Zhang, Q.:
742 Modeling Regional/Urban Ozone and Particulate Matter in Beijing, China, *J. Air*
743 *Waste Manage.*, 59, 37-44, 2009.

744 Fu, T. M., Jacob, D. J., Palmer, P. I., Chance, K., Wang, Y. X. X., Barletta, B., Blake,
745 D. R., Stanton, J. C., and Pilling, M. J.: Space-based formaldehyde measurements
746 as constraints on volatile organic compound emissions in east and south Asia and
747 implications for ozone, *J. Geophys. Res.*, 112, D06312, doi:
748 10.1029/2006JD007853, 2007.

749 Fu, T.-M., Jacob D. J., Wittrock, F., Burrows, J. P., Vrekoussis, M., and Henze, D. K.:
750 Global budgets of atmospheric glyoxal and methylglyoxal, and implications for
751 formation of secondary organic aerosols, *J. Geophys. Res.*, 113, D15303,
752 doi:10.1026/2007JD009505, 2008.

753 Gery, M. W., Whitten, G. Z., Killus, J. P., and Dodge, M. C.: A photochemical kinetics
754 mechanism for urban and regional scale computer modeling, *J. Geophys. Res.*, 94,
755 12925–12956, 1989

756 Goliff, W. S., Stockwell, W. R., and Lawson, C. V.: The regional atmospheric
757 chemistry mechanism, version 2, *Atmos. Environ.*, 68, 174–185, 2013.

758 Guenther, A. B., Jiang, X., Heald, C. L., Sakulyanontvittaya, T., Duhl, T., Emmons, L.
759 K., and Wang, X.: The Model of Emissions of Gases and Aerosols from Nature
760 version 2.1 (MEGAN2.1): an extended and updated framework for modeling
761 biogenic emissions, *Geosci. Model Dev.*, 5, 1471-1492,
762 doi:10.5194/gmd-5-1471-2012, 2012.

763 Hogrefe, C., Lynn, B., Civerolo, K., Ku, J. Y., Rosenthal, J., Rosenzweig, C.,
764 Goldberg, R., Gaffin, S., Knowlton, K., and Kinney, P. L.: Simulating changes in
765 regional air pollution over the eastern United States due to changes in global and
766 regional climate and emissions, *J. Geophys. Res.*, 109, D22301, doi:
767 10.1029/2004jd004690, 2004.

768 Hopkins, J. R., Lewis, A. C., and Read, K. A.: A two-column method for long-term
769 monitoring of non-methane hydrocarbons (NMHCs) and oxygenated volatile
770 organic compounds (o-VOCs), *J. Environ. Monitor.*, 5, 8-13, doi:
771 10.1039/b202798d, 2003.

772 Houyoux, M. R., Vukovich, J. M., Coats, C. J., Wheeler, N. J. M., and Kasibhatla, P.
773 S.: Emission inventory development and processing for the Seasonal Model for
774 Regional Air Quality (SMRAQ) project, *J. Geophys. Res.*, 105, 9079-9090, 2000.

775 Hsu, Y. and Divita, F.: SPECIATE 4.2, speciation database development
776 documentation, final report, EPA/600-R-09/-38, 2009.

777 Huang, Y., Ho, S. S. H., Ho, K. F., Lee, S. C., Yu, J. Z., and Louie, P. K. K.:
778 Characteristics and health impacts of VOCs and carbonyls associated with
779 residential cooking activities in Hong Kong, *J. Hazard. Mater.*, 186, 344-351,
780 2011.

781 Kelly, T. J. and Holdren, M. W.: Applicability of canisters for sample storage in the
782 determination of hazardous air pollutants, *Atmos. Environ.*, 29, 2595-2608, 1995.

783 Kim, Y., Couvidat, F., Sartelet, K., and Seigneur, C.: Comparison of different
784 gas-phase mechanisms and aerosol modules for simulating particulate matter
785 formation, *J. Air Waste Manage.*, 61, 1218-1226, 2011.

786 Klimont, Z., Streets, D. G., Gupta, S., Cofala, J., Fu, L. X., and Ichikawa, Y.:
787 Anthropogenic emissions of non-methane volatile organic compounds in China,
788 *Atmos. Environ.*, 36, 1309-1322, 2002.

789 Lai, C. H., Chang, C. C., Wang, C. H., Shao, M., Zhang, Y. H., and Wang, J. L.:
790 Emissions of liquefied petroleum gas (LPG) from motor vehicles, *Atmos.*
791 *Environ.*, 43, 1456-1463, 2009.

792 Lamarque, J.-F., Bond, T. C., Eyring, V., Granier, C., Heil, A., Klimont, Z., Lee, D.,
793 Liousse, C., Mieville, A., Owen, B., Schultz, M. G., Shindell, D., Smith, S. J.,
794 Stehfest, E., Van Aardenne, J., Cooper, O. R., Kainuma, M., Mahowald, N.,
795 McConnell, J. R., Naik, V., Riahi, K., and van Vuuren, D. P.: Historical (1850–

796 2000) gridded anthropogenic and biomass burning emissions of reactive gases and
797 aerosols: methodology and application, *Atmos. Chem. Phys.*, 10, 7017-7039,
798 doi:10.5194/acp-10-7017-2010, 2010.

799 Lin, M., Fiore, A. M., Horowitz, L. W., Cooper, O. R., Naik, V., Holloway, J., Johnson,
800 B. J., Middlebrook, A. M., Oltmans, S. J., Pollack, I. B., Ryerson, T. B., Warner, J.
801 X., Wiedinmyer, C., Wilson, J., and Wyman, B.: Transport of Asian ozone
802 pollution into surface air over the western United States in spring, *J. Geophys.*
803 *Res.*, 117, D00V07, doi: 10.1029/2011JD016961, 2012.

804 Liu, Y., Shao, M., Fu, L. L., Lu, S. H., Zeng, L. M., and Tang, D. G.: Source profiles
805 of volatile organic compounds (VOCs) measured in China: Part I, *Atmos.*
806 *Environ.*, 42, 6247-6260, 2008a.

807 Liu, Y., Shao, M., Lu, S., Chang, C.-C., Wang, J.-L., and Fu, L.: Source
808 apportionment of ambient volatile organic compounds in the Pearl River Delta,
809 China: Part II, *Atmos. Environ.*, 42, 6261-6274, 2008b.

810 Liu, Z., Wang, Y., Vrekoussis, M., Richter, A., Wittrock, F., Burrows, J. P., Shao, M.,
811 Chang, C.-C., Liu, S.-C., Wang, H., and Chen, C.: Exploring the missing source of
812 glyoxal (CHOCHO) over China, *Geophys. Res. Lett.*, 39, L10812, doi:
813 10.1029/2012GL051645, 2012.

814 Lu, H. X., Wen, S., Feng, Y. L., Wang, X. N., Bi, X. H., Sheng, G. Y., and Fu, J. M.:
815 Indoor and outdoor carbonyl compounds and BTEX in the hospitals of
816 Guangzhou, China, *Sci. Total Environ.*, 368, 574-584, 2006.

817 Na, K., Kim, Y. P., Moon, I., and Moon, K. C.: Chemical composition of major VOC
818 emission sources in the Seoul atmosphere, *Chemosphere*, 55, 585-594, 2004.

819 Piccot, S. D., Watson, J. J., and Jones, J. W.: A global inventory of volatile organic
820 compound emissions from anthropogenic sources, *J. Geophys. Res.*, 97,
821 9897-9912, 1992.

822 Reff, A., Bhave, P. V., Simon, H., Pace, T. G., Pouliot, G. A., Mobley, J. D., and
823 Houyoux, M.: Emissions Inventory of PM_{2.5} Trace Elements across the United

824 States, *Environ. Sci. Technol.*, 43, 5790-5796, 2009.

825 Schauer, J. J., Kleeman, M. J., Cass, G. R., and Simoneit, B. R. T.: Measurement of
826 emissions from air pollution sources. 2. C-1 through C-30 organic compounds
827 from medium duty diesel trucks, *Environ. Sci. Technol.*, 33, 1578-1587, 1999.

828 Schauer, J. J., Kleeman, M. J., Cass, G. R., and Simoneit, B. R. T.: Measurement of
829 emissions from air pollution sources. 3. C-1-C-29 organic compounds from
830 fireplace combustion of wood, *Environ. Sci. Technol.*, 35, 1716-1728, 2001.

831 Schauer, J. J., Kleeman, M. J., Cass, G. R., and Simoneit, B. R. T.: Measurement of
832 emissions from air pollution sources. 5. C-1-C-32 organic compounds from
833 gasoline-powered motor vehicles, *Environ. Sci. Technol.*, 36, 1169-1180, 2002.

834 Simon, H., Beck, L., Bhave, P. V., Divita, F., Hsu, Y., Luecken, D., Mobley, J. D.,
835 Pouliot, G. A., Reff, A., Sarwar, G., and Strum, M.: The development and uses of
836 EPA's SPECIATE database, *Atmos. Pollut. Res.*, 1, 196-206, 2010.

837 Song, Y., Shao, M., Liu, Y., Lu, S., Kuster, W., Goldan, P., and Xie, S.: Source
838 Apportionment of Ambient Volatile Organic Compounds in Beijing, *Environ. Sci.*
839 *Technol.*, 41, 4348-4353, 2007.

840 Stockwell W. R., Middleton, P., Chang, J. S., and Tang, X.: The second generation
841 Regional Acid Deposition Model chemical mechanism for regional air quality
842 modeling, *J. Geophys. Res.*, 95, 16343-16367, 1990.

843 Stockwell, W. R., Kirchner, F., Kuhn, M., and Seefeld, S.: A new mechanism for
844 regional atmospheric chemistry modeling, *J. Geophys. Res.*, 102, 25847-25879,
845 1997.

846 Streets, D. G., Bond, T. C., Carmichael, G. R., Fernandes, S. D., Fu, Q., He, D.,
847 Klimont, Z., Nelson, S. M., Tsai, N. Y., Wang, M. Q., Woo, J. H., and Yarber, K. F.:
848 An inventory of gaseous and primary aerosol emissions in Asia in the year 2000, *J.*
849 *Geophys. Res.*, 108, 8809, doi: 10.1029/2002JD003093, 2003.

850 Tang, J. H., Chan, L. Y., Chan, C. Y., Li, Y. S., Chang, C. C., Wang, X. M., Zou, S. C.,
851 Barletta, B., Blake, D. R., and Wu, D.: Implications of changing urban and rural

852 emissions on non-methane hydrocarbons in the Pearl River Delta region of China,
853 Atmos. Environ., 42, 3780-3794, 2008.

854 Tsai, S. M., Zhang, J. F., Smith, K. R., Ma, Y. Q., Rasmussen, R. A., and Khalil, M. A.
855 K.: Characterization of non-methane hydrocarbons emitted from various
856 cookstoves used in China, Environ. Sci. Technol., 37, 2869-2877, 2003.

857 US EPA: Guidance on the use of models and other analyses for demonstrating
858 attainment of air quality for ozone, PM_{2.5} and regional haze, US Environmental
859 Protection Agency, United States, 253 pp., 2007.

860 van der Werf, G. R., Randerson, J. T., Giglio, L., Collatz, G. J., Mu, M., Kasibhatla, P.
861 S., Morton, D. C., DeFries, R. S., Jin, Y., and van Leeuwen, T. T.: Global fire
862 emissions and the contribution of deforestation, savanna, forest, agricultural, and
863 peat fires (1997-2009), Atmos. Chem. Phys., 10, 11707-11735, doi:
864 10.5194/acp-11707-2010, 2010.

865 Wang, L., Jang, C., Zhang, Y., Wang, K., Zhang, Q., Streets, D., Fu, J., Lei, Y.,
866 Schreifels, J., He, K., Hao, J., Lam, Y.-F., Lin, J., Meskhidze, N., Voorhees, S.,
867 Evarts, D., and Phillips, S.: Assessment of air quality benefits from national air
868 pollution control policies in China. Part II: Evaluation of air quality predictions and
869 air quality benefits assessment, Atmos. Environ., 44, 3449-3457, 2010.

870 Wang, M., Shao, M., Chen, W., Yuan, B., Lu, S., Zhang, Q., Zeng, L., and Wang, Q.:
871 Validation of emission inventories by measurements of ambient volatile organic
872 compounds in Beijing, China, Atmos. Chem. Phys. Discuss., 13, 26933-26979,
873 doi: 10.5194/acpd-13-26933-2013, 2013.

874 Wang, S., Wei, W., Du, L., Li, G., and Hao, J.: Characteristics of gaseous pollutants
875 from biofuel-stoves in rural China, Atmos. Environ., 43, 4148-4154, 2009.

876 Wang, X. M., Sheng, G. Y., Fu, J. M., Chan, C. Y., Lee, S. G., Chan, L. Y., and Wang,
877 Z. S.: Urban roadside aromatic hydrocarbons in three cities of the Pearl River
878 Delta, People's Republic of China, Atmos. Environ., 36, 5141-5148, 2002.

879 Wang, Y., Zhang, Y., Hao, J., and Luo, M.: Seasonal and spatial variability of surface

880 ozone over China: contributions from background and domestic pollution, *Atmos.*
881 *Chem. Phys.*, 11, 3511-3525, 2011.

882 Wei, W., Wang, S. X., Chatani, S., Klimont, Z., Cofala, J., and Hao, J. M.: Emission
883 and speciation of non-methane volatile organic compounds from anthropogenic
884 sources in China, *Atmos. Environ.*, 42, 4976-4988, 2008.

885 Wittrock, F., Richter, A., Oetjen, H., Burrows, J. P., Kanakidou, M., Myriokefalitakis,
886 S., Volkamer, R., Beirle, S., Platt, U., and Wagner, T.: Simultaneous global
887 observations of glyoxal and formaldehyde from space, *Geophys. Res. Lett.*, 33,
888 L16804, doi: 10.1029/2006GL026310, 2006.

889 Woo, J. H., Baek, J. M., Kim, J. W., Carmichael, G. R., Thongboonchoo, N., Kim, S.
890 T., and An, J. H.: Development of a multi-resolution emission inventory and its
891 impact on sulfur distribution for Northeast Asia, *Water Air Soil Poll.*, 148,
892 259-278, 2003.

893 Xing, J., Zhang, Y., Wang, S., Liu, X., Cheng, S., Zhang, Q., Chen, Y., Streets, D. G.,
894 Jang, C., Hao, J., and Wang, W.: Modeling study on the air quality impacts from
895 emission reductions and atypical meteorological conditions during the 2008
896 Beijing Olympics, *Atmos. Environ.*, 45, 1786-1798, 2011.

897 Yarwood, G., Rao, S., Yocke, M., and Whitten, G.: Updates to the Carbon Bond
898 Chemical Mechanism: CB05, Final Report to the US EPA, RT-0400675, available
899 at: <http://www.camx.com> (last access: October 2013), 2005.

900 Yuan, B., Shao, M., Lu, S., and Wang, B.: Source profiles of volatile organic
901 compounds associated with solvent use in Beijing, China, *Atmos. Environ.*, 44,
902 1919-1926, 2010.

903 Zaveri, R. A. and Peters, L. K.: A new lumped structure photochemical mechanism for
904 large-scale applications, *J. Geophys. Res.*, 104, 30387-30415, doi:
905 10.1029/1999JD900876, 1999.

906 Zhang, Q., Streets, D. G., Carmichael, G. R., He, K. B., Huo, H., Kannari, A.,
907 Klimont, Z., Park, I. S., Reddy, S., Fu, J. S., Chen, D., Duan, L., Lei, Y., Wang, L.

908 T., and Yao, Z. L.: Asian emissions in 2006 for the NASA INTEX-B mission,
909 Atmos. Chem. Phys., 9, 5131-5153, doi: 10.5194/acp-9-5131-2009, 2009.

910 Zhang, Y., Liu, X.-H., Olsen, K. M., Wang, W.-X., Do, B. A., and Bridgers, G. M.:
911 Responses of future air quality to emission controls over North Carolina, Part II:
912 Analyses of future-year predictions and their policy implications, Atmos. Environ.,
913 44, 2767-2779, 2010.

914 Zhang, Y., Chen, Y., Sarwar, G., and Schere, K.: Impact of gas-phase mechanisms on
915 Weather Research Forecasting Model with Chemistry (WRF/Chem) predictions:
916 Mechanism implementation and comparative evaluation, J. Geophys. Res., 117,
917 D01301, doi: 10.1029/2011jd015775, 2012.

918 Zhang, Y., Wang, W., Wu, S.-Y., Kang, K., Minoura, H., and Wang, Z.-F.: Impacts of
919 updated emission inventories on source apportionment of fine particle and ozone
920 over the southeastern US, Atmos. Environ., under review, 2013.

921 Zhang, Y.L., Wang, X.M., Zhang, Z., Lu S.J., Shao, M., Lee, F.S.C., and Yu, J.Z.:
922 Species profiles and normalized reactivity of volatile organic compounds from
923 gasoline evaporation in China, Atmos. Environ., 79, 110-118, 2013.

924 Zhao, L. R., Wang, X. M., He, Q. S., Wang, H., Sheng, G. Y., Chan, L. Y., Fu, J. M.,
925 and Blake, D. R.: Exposure to hazardous volatile organic compounds, PM10 and
926 CO while walking along streets in urban Guangzhou, China, Atmos. Environ., 38,
927 6177-6184, 2004.

928 Zheng, J. Y., Shao, M., Che, W. W., Zhang, L. J., Zhong, L. J., Zhang, Y. H., and
929 Streets, D.: Speciated VOC Emission Inventory and Spatial Patterns of Ozone
930 Formation Potential in the Pearl River Delta, China, Environ. Sci. Technol., 43,
931 8580-8586, 2009.

932

Table 1. NMVOC emission inventories covering Asian regions

Inventory	Source ^a	Region	Year	Species included	Profiles used
EDGAR v2 ^b	AN+BB	Global	1990	23 groups	Unknown
EDGAR v3 ^c and v4 ^d	AN+BB	Global	1970-2008	N/A	
POET ^e	AN+BB	Global	1990-2000	13 groups	Unknown
RETRO ^f	AN+BB	Global	1960-2000	22 groups	Unknown
Lamarque et al., 2010	AN+BB	Global	1850-2000	22 groups	From RETRO
Klimont et al., 2002	AN	China	1995	16 groups	SPECIATE
Streets et al., 2003	AN+BB	Asia	2000	19 groups	SPECIATE
Ohara et al., 2007 ^g	AN+BB	Asia	1980-2003	N/A	
Kurokawa et al., 2013	AN+BB	Asia	2000-2008	19 groups	From Streets et al. (2003)
Bo et al., 2008	AN	China	1980-2005	N/A	
Wei et al., 2008	AN	China	2005	40 groups including major individual active species	Local profiles + SPECIATE
Zheng et al., 2009	AN+BG	PRD, China	2006	91 species from AN, and 30 species from BG	Local profiles + SPECIATE
Cai et al., 2009	Transportation	China	1980-2005	67 species	From literatures
This work	AN	Asia	2006	~700 individual species; then mapping to emitting species of 8 chemical mechanisms	

^aAN = anthropogenic; BB = biomass burning; BG = biogenic.

^bavailable at: http://www.pbl.nl/en/themasites/geia/emissions_data/nmvoc_groups/index.html.

^cavailable at: http://themasites.pbl.nl/tridion/en/themasites/edgar/emission_data/edgar32/index-2.html.

^davailable at: <http://edgar.jrc.ec.europa.eu/index.php>; <http://eccad.sedoo.fr>.

^eavailable at: <http://www.aero.jussieu.fr/projet/ACCENT/POET.php>; <http://eccad.sedoo.fr>.

^favailable at: http://retro.enes.org/data_emissions.shtml.

^gnot independent estimates. Data extrapolated from Klimont et al., 2002 and Streets et al., 2003.

Table 2. Mapping table from SAPRC-99 species to GEOS-Chem Species.

SAPRC-99	GEOS-Chem
ACET	ACET
CCHO	ALD2
ALK3+ALK4+ALK5	ALK4
ALK1	C2H6
ALK2	C3H8
HCHO	CH2O
MEK	MEK
OLE1+OLE2	PRPE

Table 3. Mapping table from SAPRC-99 species to MOZART-4 Species.

SAPRC-99	MOZART-4
ALK3 ^a +ALK4+ALK5	BIGALK
OLE2	BIGENE
ARO1+ARO2	TOLUENE
OLE1	C3H6
ALK2	C3H8
ALK1	C2H6
ETHE	C2H4
MEK+PRD2	MEK
HCHO	CH2O
CCHO	CH3CHO
ACET	CH3COCH3
MEOH	CH3OH
Not available	C2H5OH ^b

^a Ethyl alcohol is removed from ALK3 when mapping to BIGALK.

^b Taken from ethyl alcohol emissions.

Table 4. Spatial proxies used in this work.

Source category	Spatial proxies
Large power plants (>300MW)	Location
Small power plants (<300MW)	Total population
Industry combustion	Urban population
Residential boilers	Urban population
Residential biofuel	Rural population
On-road transportation	Road network
Off-road transportation	Rural population
All other sources	Total population

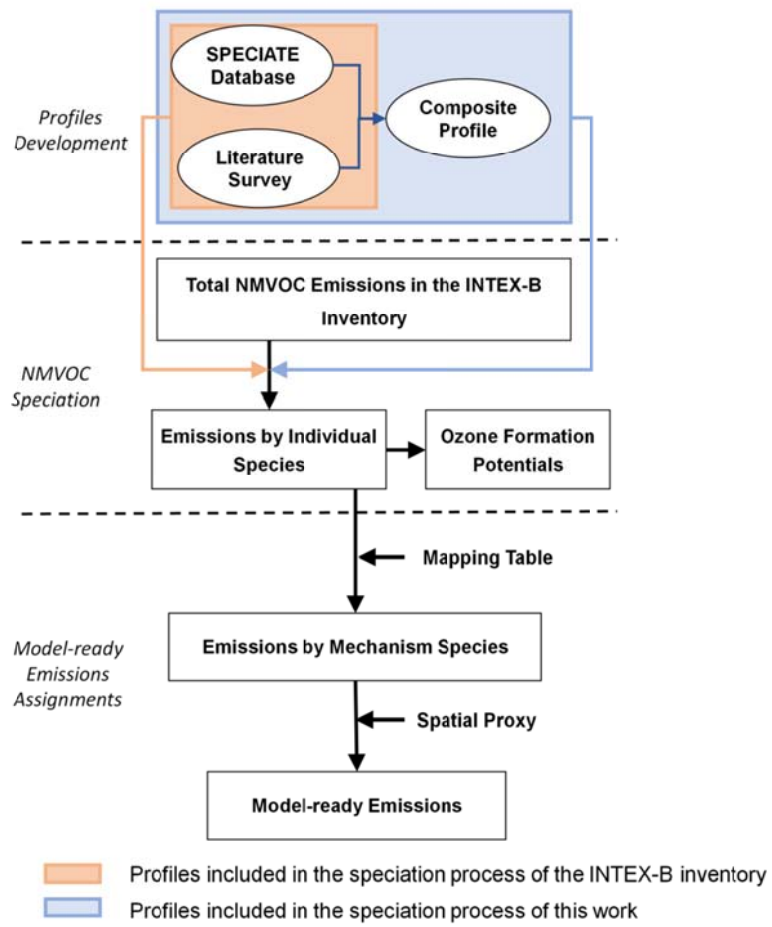


Fig. 1. Schematic methodology of this study.

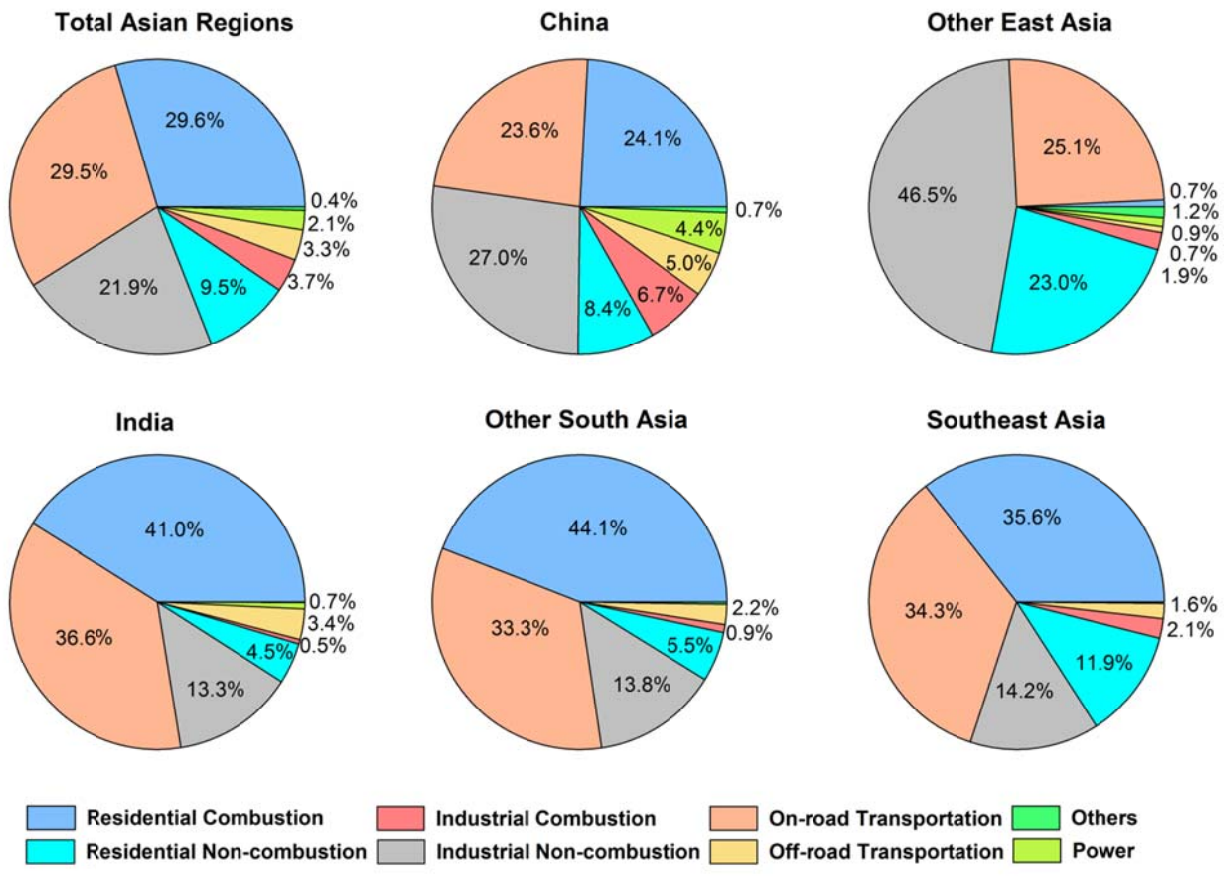


Fig. 2. 2006 NMVOC emissions by Asian regions in the INTEX-B inventory.

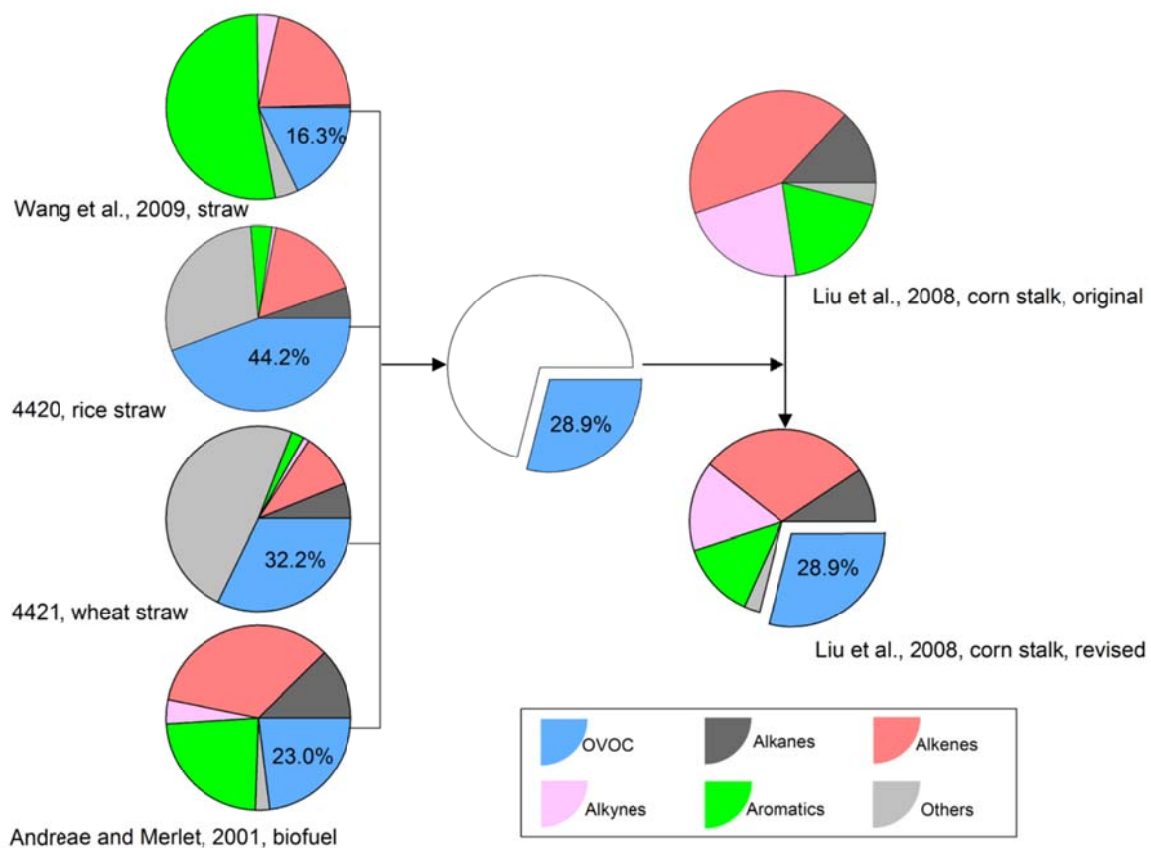


Fig. 3. Inclusion of OVOC fraction for incomplete crop residue combustion profiles. 4420 and 4421 are the “P_NUMBER”s of profiles taken from the SPECIATE database developed by the US EPA.

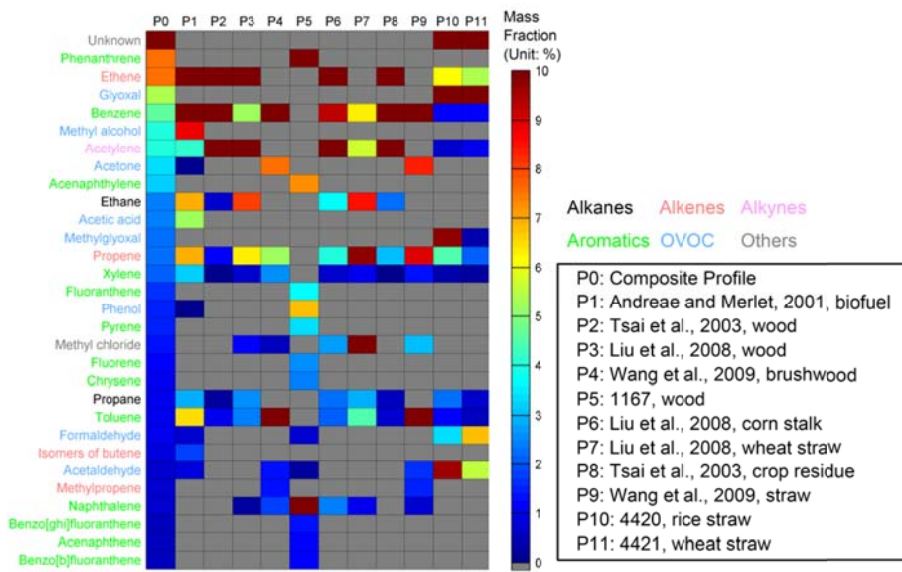


Fig. 4. Mass fraction of major species in the profiles for the residential biofuel combustion. Top 30 species are presented and ranked decreasingly based on the mass fraction in the composite profile (P0). Grey grids indicate that mass fractions for these species are not included in the profile.

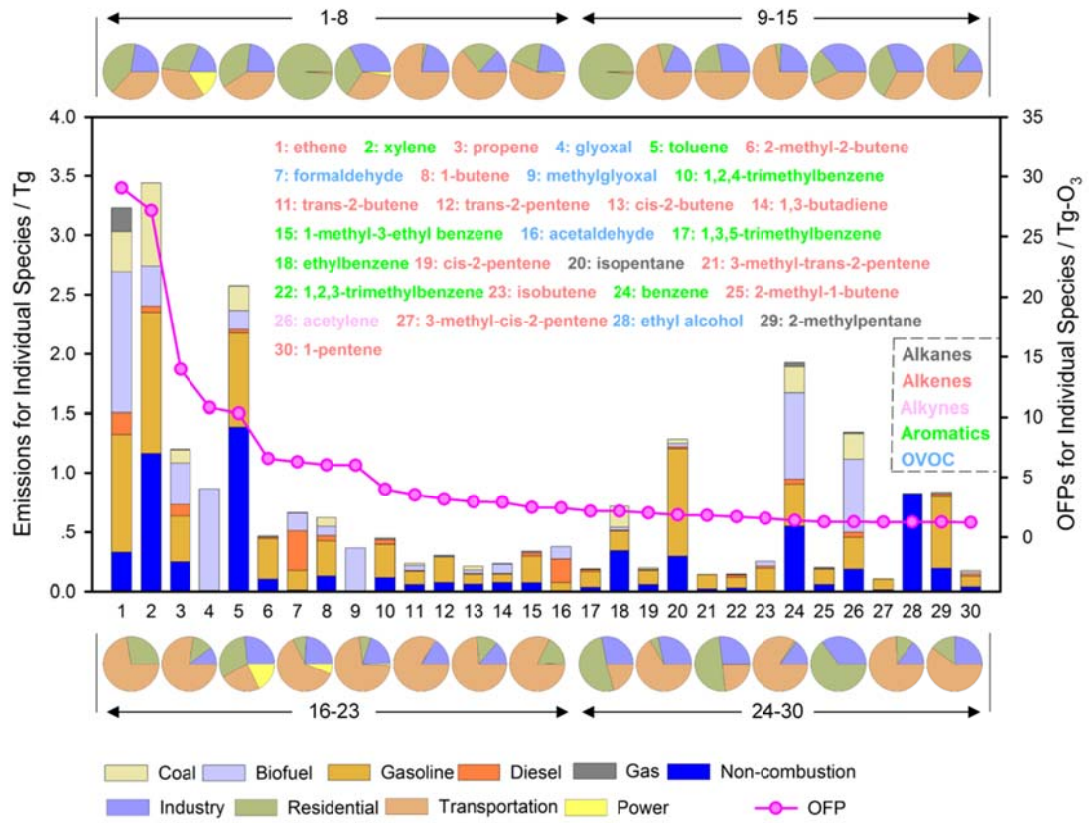


Fig. 5. Emissions by individual NMVOC species and corresponding OFPs.

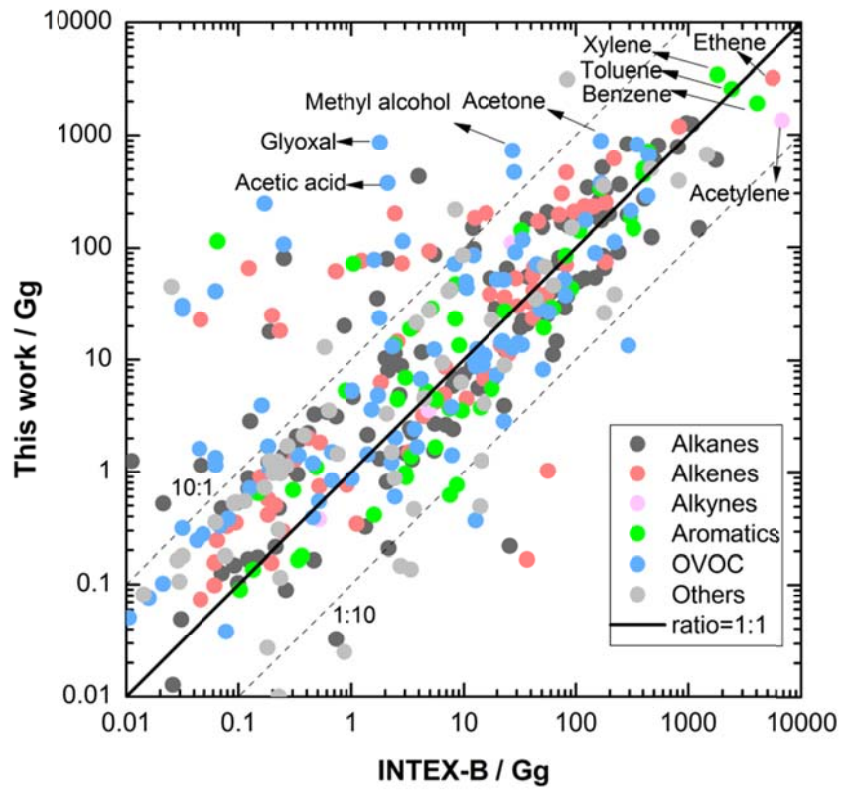


Fig. 6. Comparison of this work and the INTEX-B inventory by individual species.

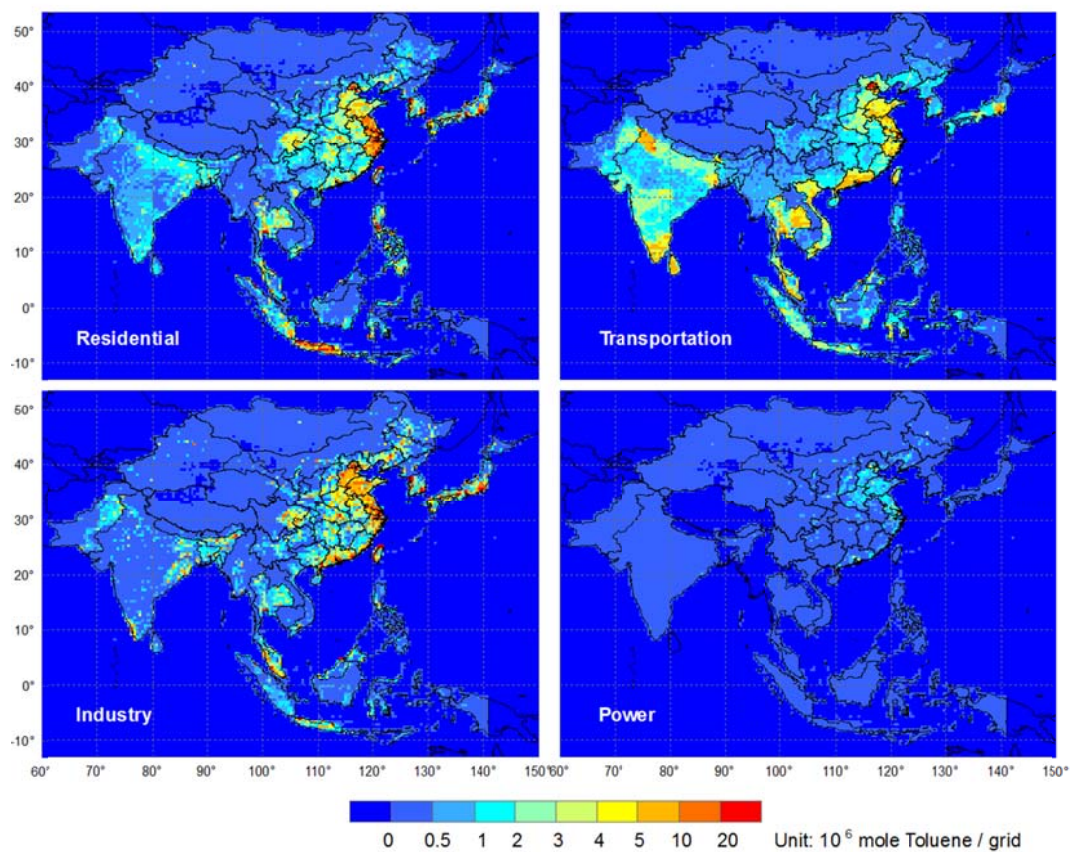


Fig. 7. Emission distribution of toluene by sector at 30 min × 30 min resolution (unit: 10⁶ mole yr⁻¹ per grid).

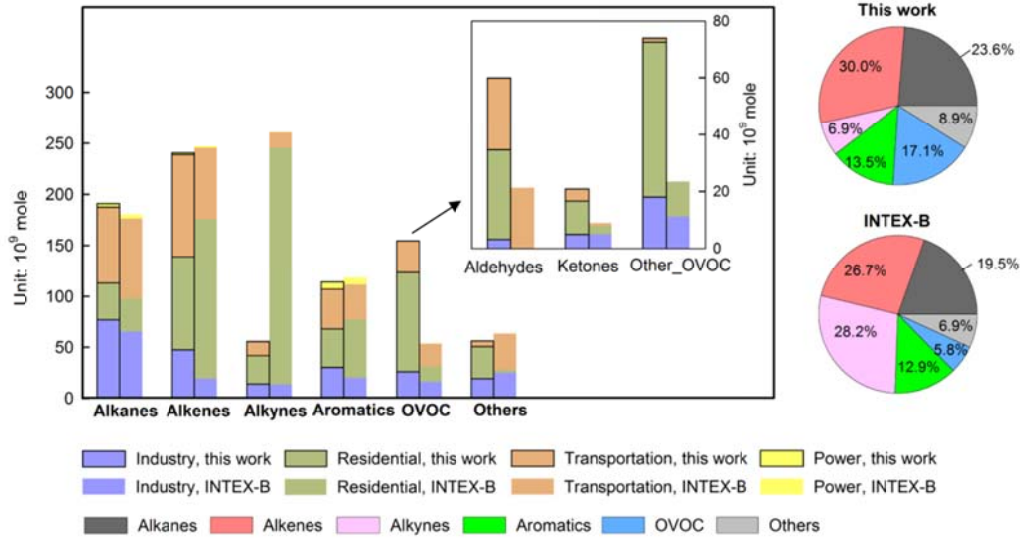


Fig. 8. Asian anthropogenic NMVOC emissions in 2006 by chemical groups.

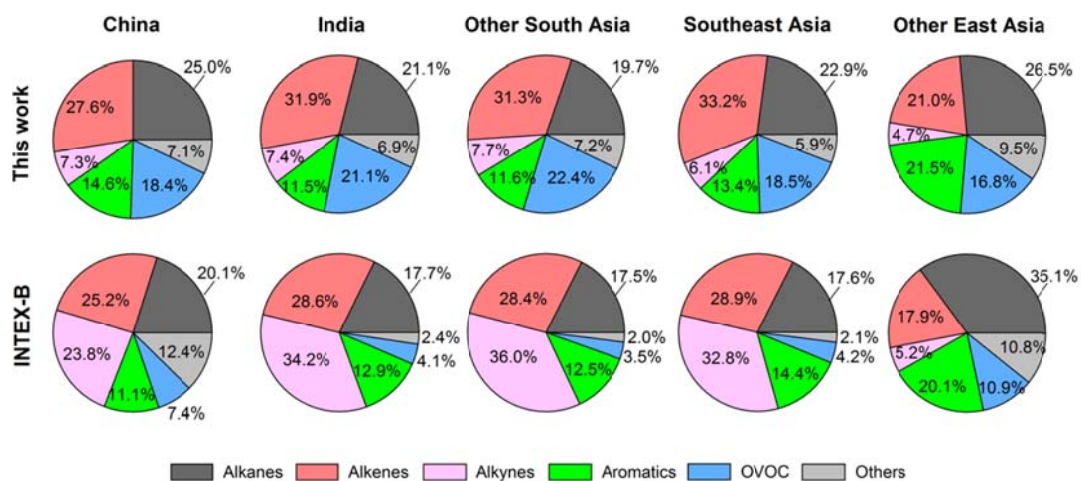
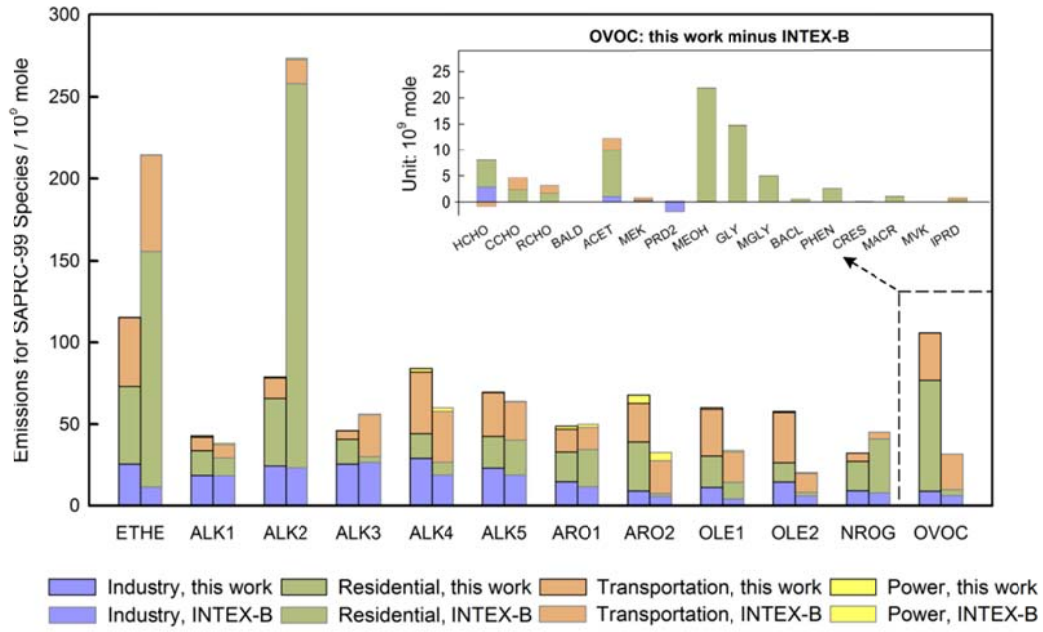
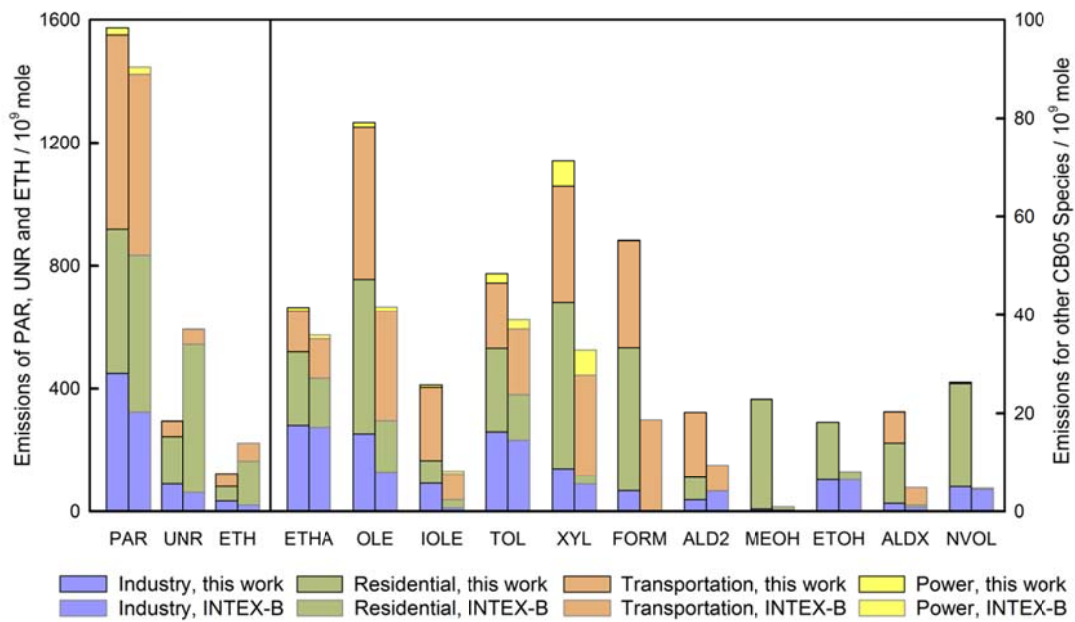


Fig. 9. Distribution of anthropogenic NMVOC emissions in 2006 among different chemical groups for Asia regions.



(a) SAPRC-99



(b) CB05

Fig. 10. 2006 Asian anthropogenic NMVOC emissions by SAPRC-99 (a) and CB05 (b) species. An explanation of the abbreviations of SAPRC-99 and CB05 emitting species are presented in Tables A1 and A2.

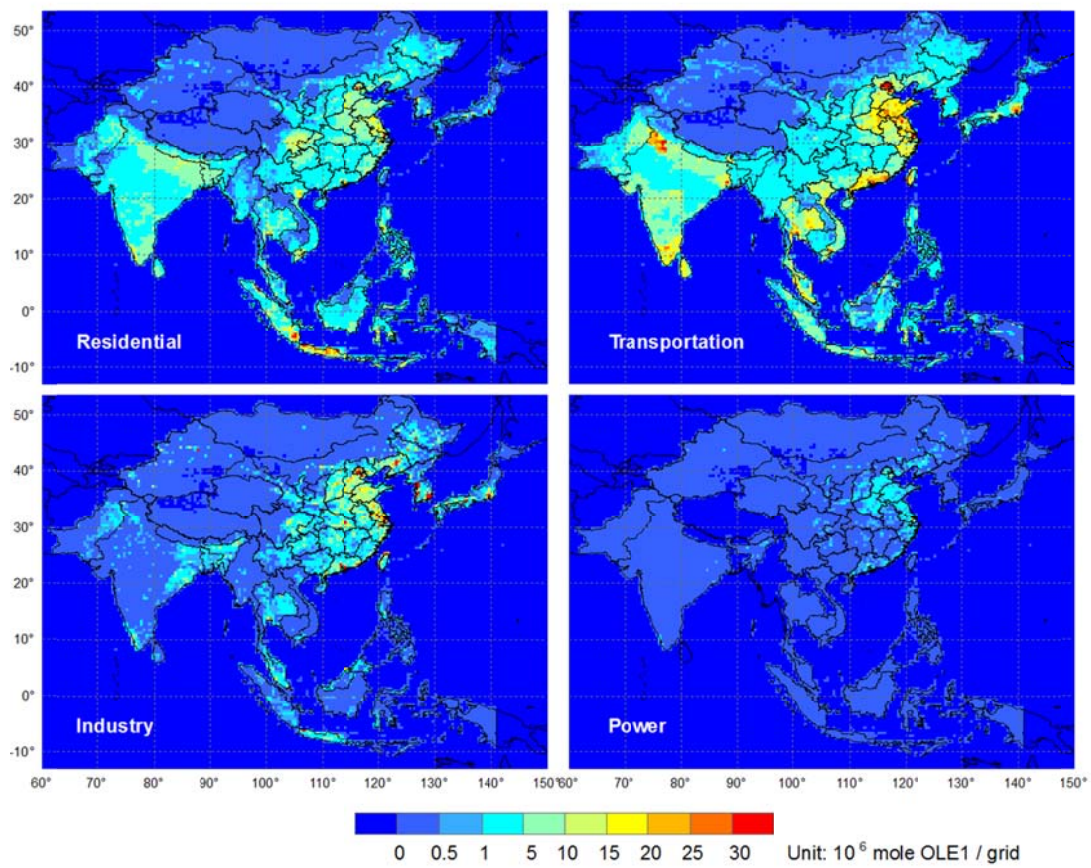


Fig. 11. Emission distribution at $30 \text{ min} \times 30 \text{ min}$ resolution of OLE1, SAPRC-99 species.

Emissions for SAPRC-99 species

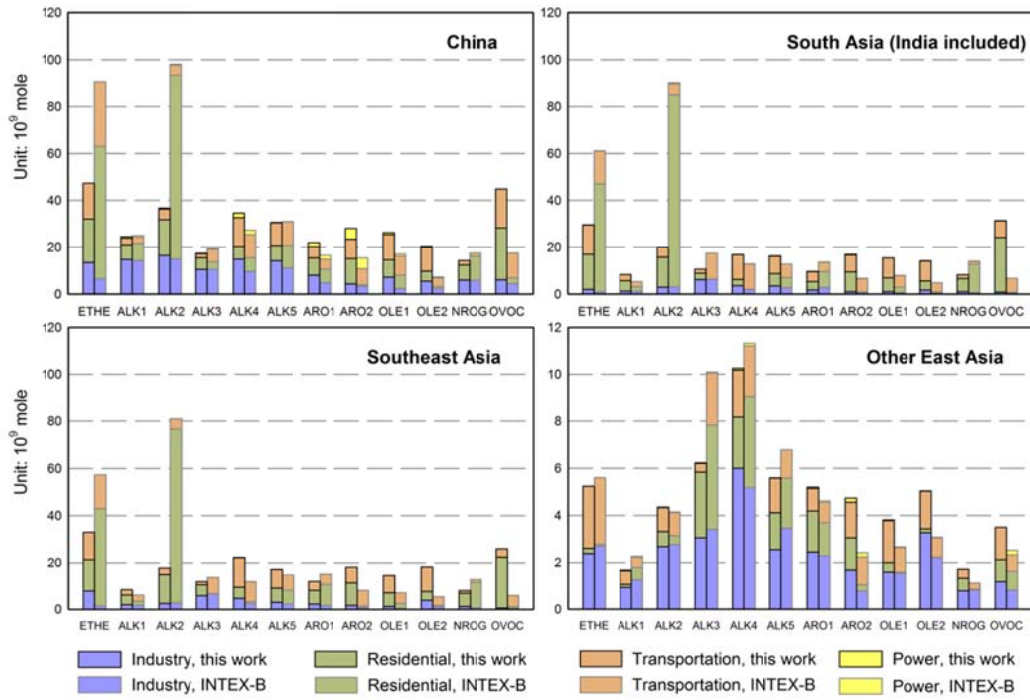


Fig. 12. 2006 Asian emissions for SAPRC-99 mechanism species by regions.

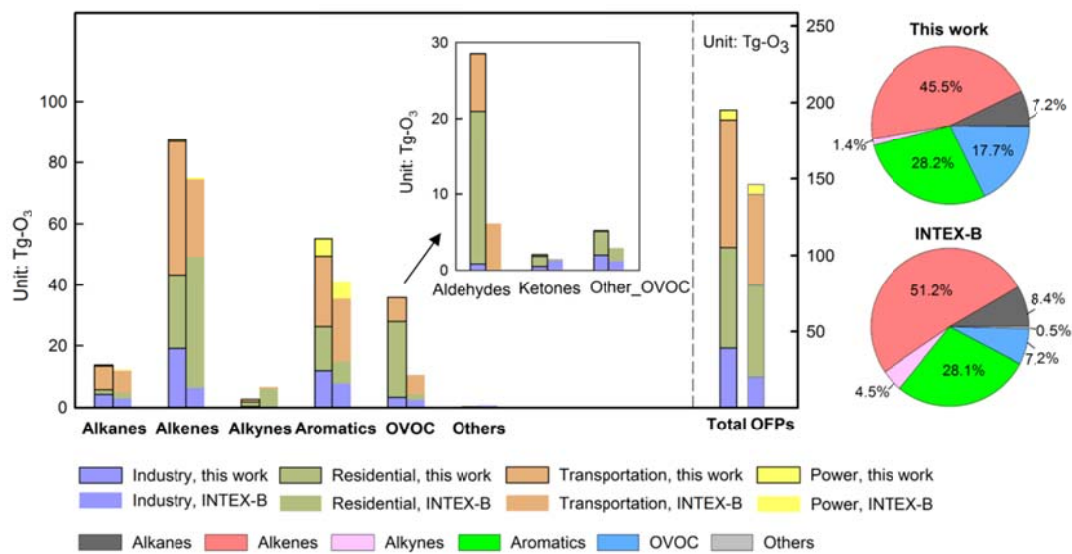


Fig. 13. Ozone Formation Potentials (OFP) of Asian anthropogenic NMVOC emissions in 2006 by chemical groups.

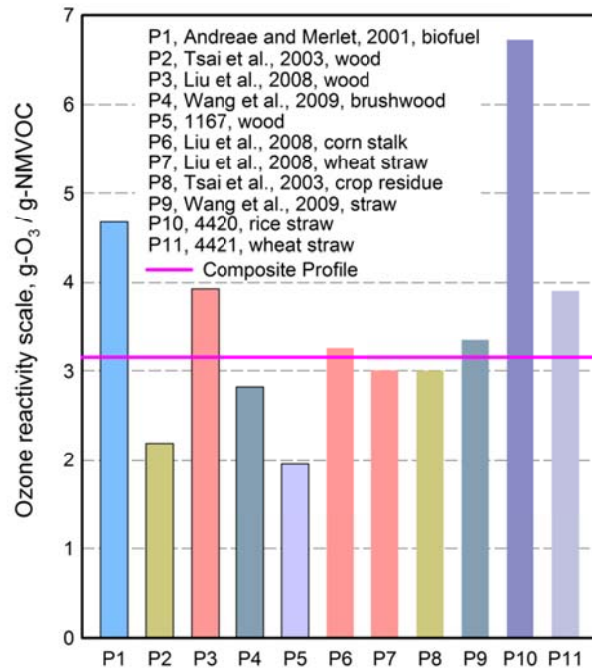


Fig. 14. Sensitivity of OFPs to profile selection for the residential biofuel combustion.

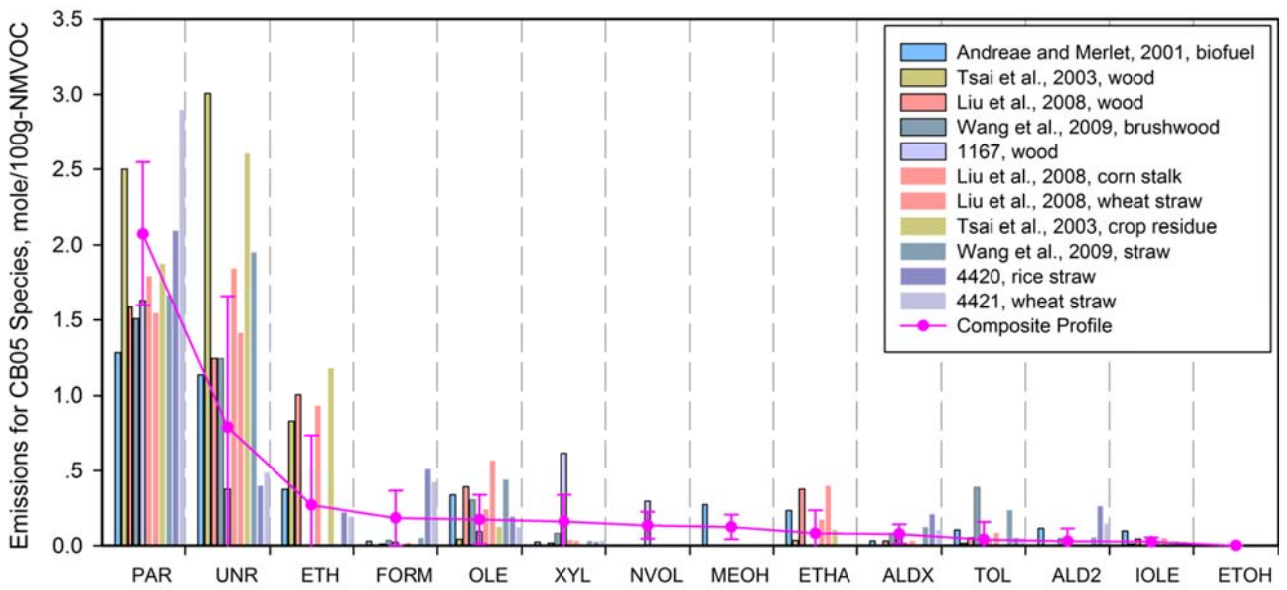
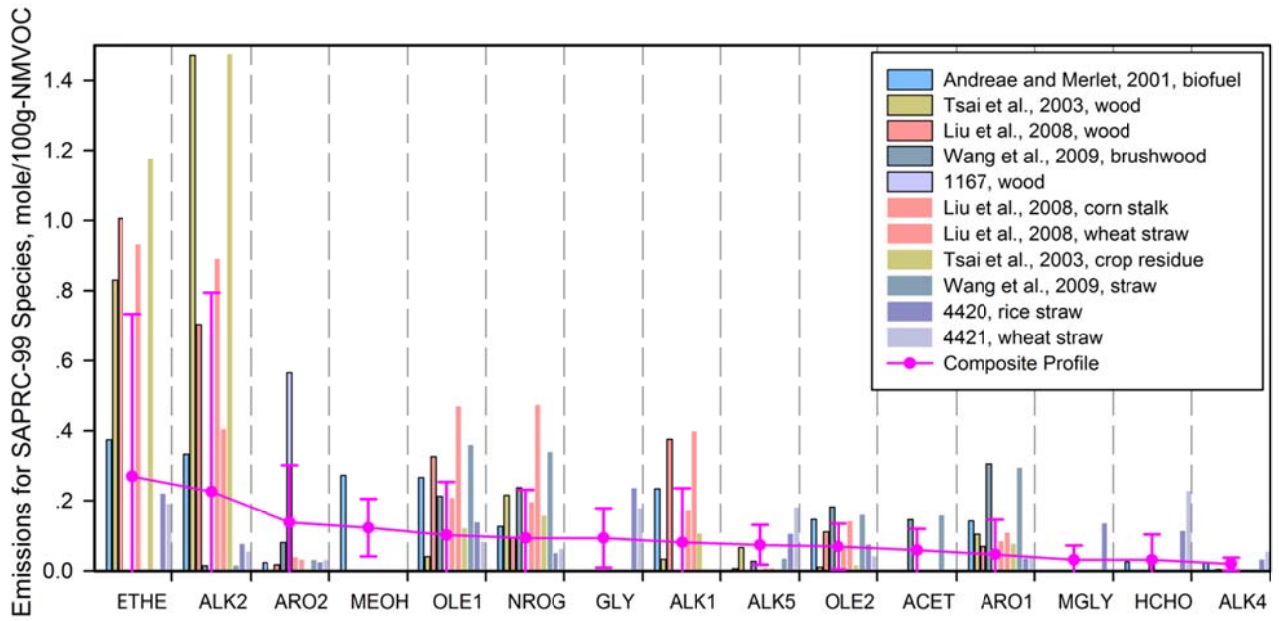


Fig. 15. Sensitivity of model-ready emissions to profile selection for the residential biofuel combustion.